

Spring 2006

## Magnetic Coupling between a “Hot Jupiter” Extrasolar Planet and Its Pre-Main-Sequence Central Star

Brooke E. Alarcon

*Embry-Riddle Aeronautical University - Daytona Beach*

Follow this and additional works at: <https://commons.erau.edu/db-theses>



Part of the [Atmospheric Sciences Commons](#), and the [Physics Commons](#)

---

### Scholarly Commons Citation

Alarcon, Brooke E., "Magnetic Coupling between a “Hot Jupiter” Extrasolar Planet and Its Pre-Main-Sequence Central Star" (2006). *Theses - Daytona Beach*. 23.

<https://commons.erau.edu/db-theses/23>

This thesis is brought to you for free and open access by Embry-Riddle Aeronautical University – Daytona Beach at ERAU Scholarly Commons. It has been accepted for inclusion in the Theses - Daytona Beach collection by an authorized administrator of ERAU Scholarly Commons. For more information, please contact [commons@erau.edu](mailto:commons@erau.edu).

MAGNETIC COUPLING BETWEEN A  
“HOT JUPITER” EXTRASOLAR PLANET AND  
ITS PRE-MAIN-SEQUENCE CENTRAL STAR

By

Brooke E. Alarcón

A thesis Submitted to the  
Physical Science Department  
in Partial Fulfillment of the Requirements for the Degree of  
Master of Science in Space Science

Embry-Riddle Aeronautical University  
Daytona Beach, Florida  
Spring 2006

UMI Number: EP32031

### INFORMATION TO USERS

The quality of this reproduction is dependent upon the quality of the copy submitted. Broken or indistinct print, colored or poor quality illustrations and photographs, print bleed-through, substandard margins, and improper alignment can adversely affect reproduction.

In the unlikely event that the author did not send a complete manuscript and there are missing pages, these will be noted. Also, if unauthorized copyright material had to be removed, a note will indicate the deletion.

UMI<sup>®</sup>

---

UMI Microform EP32031  
Copyright 2011 by ProQuest LLC  
All rights reserved. This microform edition is protected against  
unauthorized copying under Title 17, United States Code.

---

ProQuest LLC  
789 East Eisenhower Parkway  
P.O. Box 1346  
Ann Arbor, MI 48106-1346

MAGNETIC COUPLING BETWEEN A  
"HOT JUPITER" EXTRASOLAR PLANET AND  
ITS PRE-MAIN-SEQUENCE CENTRAL STAR

By

Brooke E. Alarcón


This thesis was prepared under the direction of the candidate's thesis advisor, Dr. Robert C. Fleck, Jr., Physical Science Department, and has been approved by the members of her thesis committee. It was submitted in the spring of 2006 to the Physical Science Department and was accepted in partial fulfillment of the requirements for the

Degree of


Master of Science in Space Science

THESIS COMMITTEE:

Dr. Robert C. Fleck, Jr.  
ADVISOR

 2 May 2006  
SIGNATURE DATE

Dr. Mark Reynolds  
COMMITTEE MEMBER

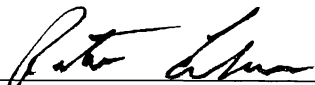
 5-2-06  
SIGNATURE DATE

Dr. Lance Erickson  
COMMITTEE MEMBER


 5/2/06  
SIGNATURE DATE

ACADEMIC DEPARTMENT AND COLLEGE:

DR. PETER W. ERDMAN  
MSSPS Graduate Program Coordinator

 5/2/06  
SIGNATURE DATE

DR. JOHN J. OLIVERO  
Department Chair, Physical Science

 5/2/06  
SIGNATURE DATE

DR. CHRISTINA M. FREDERICK-RECASCINO  
Associate Provost

 5/2/06  
SIGNATURE DATE

## Acknowledgements

First and foremost I would like to sincerely thank Dr. Robert Fleck for his guidance and inspiration in this project. His creative thought helped couple my interests in astronomy and electromagnetism to an interesting question related to a very exciting and new field of astronomy. I appreciate his assistance throughout the calculation process; it has helped me discover my own path to solving such type of problems.

In addition, as always, I would like to thank my parents and family members for always being a strong guiding force in my life. If it were not for their support over the past six years, I would not have been able to achieve my goals in academics that I have today. I must thank myself for having the patience to type up this paper, the drive to complete this Master's program, and for putting myself through the past six years of school. And finally, I have great thanks for my constant companion, my dog Athena, for always having a smile on her face and being excited to see me every day I came home tired from school.

## ABSTRACT

Title: Magnetic Coupling between a “Hot Jupiter” Extrasolar Planet and its Pre-Main-Sequence Central Star  
Author: Brooke E. Alarcón  
Institution: Embry-Riddle Aeronautical University  
Location: Daytona Beach, Florida  
Degree: Master of Science in Space Science  
Date: Spring 2006

In order to understand the short-period pile-up of extrasolar planets, the magnetic torque of a pre-main-sequence central star on a single orbiting “hot Jupiter” planet is calculated. The star’s magnetic field is modeled as a dipole magnetic field. The time-dependant stellar radius is calculated for four different stellar mass sizes;  $2M_{sun}$ ,  $1.5M_{sun}$ ,  $1M_{sun}$ , and  $0.5M_{sun}$ . The minimum planetary ionization for the giant gas planet to be nearly frozen to the magnetic field lines is calculated. The changing angular momentum of an orbiting body was balanced with the magnetic torque of the central star to provide results which support that the central star is capable of halting the migration of Type II planets. The magnetic braking effect that the planet has on the central star is enough to push out the planet during its inward migration and spin-down the star’s angular rotation. This investigation shows that the magnetic torque is a viable mechanism to explain the short period pile-up of many extrasolar planets.

# Table of Contents

<b>ACKNOWLEDGEMENTS.....</b>	<b>III</b>
<b>ABSTRACT.....</b>	<b>IV</b>
<b>TABLE OF CONTENTS.....</b>	<b>V</b>
<b>LIST OF TABLES .....</b>	<b>VI</b>
<b>LIST OF FIGURES .....</b>	<b>VII</b>
<b>I. INTRODUCTION .....</b>	<b>1</b>
<b>II. STELLAR RADIUS SIZE .....</b>	<b>10</b>
A    PARAMETERS FOR MODEL CALCULATION	10
B    CALCULATION OF STELLAR RADIUS	12
C    RESULTS	13
<b>III. TOROIDAL AND POLOIDAL MAGNETIC FIELD COMPONENTS.....</b>	<b>16</b>
<b>IV. HOT JUPITER PLANETARY IONIZATION.....</b>	<b>18</b>
A    IONIZATION BY <sup>40</sup> K AND <sup>26</sup> AL RADIOACTIVITY	19
B    IONIZATION BY X-RAYS	19
C    IONIZATION BY COSMIC RAYS	20
D    IONIZATION BY ULTRAVIOLET RADIATION	20
E    ION DENSITY	21
F    AMBIPOLAR DIFFUSION	22
<b>V. SEMIMAJOR AXIS CALCULATION.....</b>	<b>25</b>
A    TORQUE BALANCE	25
B    ANGULAR MOMENTUM EXCHANGE	28
<b>VI. RESULTS.....</b>	<b>31</b>
A    CENTRAL STAR MASS	31
B    PLANET MASS	37
C    RATIO OF POLOIDAL TO TOROIDAL MAGNETIC FIELD COMPONENTS AND MAGNETIC FLUX TUBE FOOTPRINT	41
D    ECCENTRICITY OF THE ORBITING PLANET	44
E    SURFACE MAGNETIC FIELD STRENGTH	44
F    INITIAL SEMIMAJOR AXIS	47
<b>VII. CONCLUSION .....</b>	<b>49</b>
<b>VIII. REFERENCES .....</b>	<b>51</b>
<b>APPENDIX A.....</b>	<b>52</b>
<b>APPENDIX B.....</b>	<b>61</b>
<b>APPENDIX C.....</b>	<b>66</b>
<b>APPENDIX D.....</b>	<b>68</b>

## List of Tables

Table 1. Pre-Main-Sequence Stellar Properties Modeled Using the CM Convection Model in Conjunction with Alexander's (1989) Radiative Opacity Values (D'Antona & Mazzitelli 1994). .....	11
Table 2. Pre-Main-Sequence Stellar Properties Modeled Using the CM Convection Model in Conjunction with Kurucz (1991) Radiative Opacity Values (D'Antona & Mazzeitelli 1994).....	12
Table 3. Calculated Stellar Radius Values for 17 Different Stages in its Pre-Main-Sequence Evolution. All values in $R_{\text{sun}}$ units. ....	13
Table 4. Parameter Fits for the Power Function Estimate for the Time-Dependant Stellar Radius Value. ....	14
Table 5. Gain in Angular Momentum of an Orbiting Jupiter Sized Planet Around a Solar Mass as its Semimajor Axis Increase in 0.5 AU Step-Sizes .....	30
Table 6. Planetary Properties (Schneider 2006) Updated March 11 2006. ....	53
Table 7. Stellar Properties (Schneider 2006) Updated March 11 2006. ....	56



## List of Figures

Figure 1. Extrasolar Planet $M_{sin(i)}/M_{Jup}$ Histogram.....	1
Figure 2. Distribution of Extrasolar Planet $M_{sin(i)}/M_{Jup}$ with Respect to Semimajor Axis (AU). .....	2
Figure 3. Extrasolar Planet Semimajor Axis Histogram in AU. ....	3
Figure 4. Type II Gap Forming Planet Migration (Armitage & Rice 2005). ....	4
Figure 5. Stellar Radius Evolution for Different Sized Pre-Main-Sequence Stars. Best-fit Legend: solid- $2M_{sun}$ ; dotted- $1.5M_{sun}$ ; dash/dot- $1M_{sun}$ ; dashed- $0.5M_{sun}$ . ....	15
Figure 6. Example of a Conductive Exoplanet Traveling Through the Magnetic Field Lines of the Central Star. If the Planet's Resistivity is Low Enough, it will be "Frozen" to the Field Lines. .....	18
Figure 7. The Picture shows the Area Swept Out by a Planet per Unit Time, $BCF$ , and the Perpendicular Distance $y$ from the Star to the Direction of Motion of the Planet. ....	26
Figure 8. Time Development of Semimajor Axis for a $M_{Jup}$ Size Planet about a $2M_{sun}$ Central Star for Varying Initial Semimajor Axis Positions [ $B_o = 5$ kG; $e = 0.0$ ; $\gamma = 1$ ; $\eta = 0.1$ ]. ....	33
Figure 9. Time Development of Semimajor Axis for a $M_{Jup}$ Size Planet about a $1.5M_{sun}$ Central Star for Varying Initial Semimajor Axis Positions [ $B_o = 5$ kG; $e = 0.0$ ; $\gamma = 1$ ; $\eta = 0.1$ ]. ....	34
Figure 10. Time Development of Semimajor Axis for a $M_{Jup}$ Size Planet about a $M_{sun}$ Central Star for Varying Initial Semimajor Axis Positions [ $B_o = 5$ kG; $e = 0.0$ ; $\gamma = 1$ ; $\eta = 0.1$ ]. ....	35
Figure 11. Time Development of Semimajor Axis for a $M_{Jup}$ Size Planet about a $0.5M_{sun}$ Central Star for Varying Initial Semimajor Axis Positions [ $B_o = 5$ kG; $e = 0.0$ ; $\gamma = 1$ ; $\eta = 0.1$ ]. ....	36
Figure 12. Time Development of Semimajor Axis for a $10M_{Jup}$ Size Planet about a $M_{sun}$ Central Star for Varying Initial Semimajor Axis Positions [ $B_o = 5$ kG; $e = 0.0$ ; $\gamma = 1$ ; $\eta = 0.1$ ]. ....	38
Figure 13. Time Development of Semimajor Axis for a $5M_{Jup}$ Size Planet about a $M_{sun}$ Central Star for Varying Initial Semimajor Axis Positions [ $B_o = 5$ kG; $e = 0.0$ ; $\gamma = 1$ ; $\eta = 0.1$ ]. ....	39
Figure 14. Time Development of Semimajor Axis for a $0.1M_{Jup}$ Size Planet about a $M_{sun}$ Central Star for Varying Initial Semimajor Axis Positions [ $B_o = 5$ kG; $e = 0.0$ ; $\gamma = 1$ ; $\eta = 0.1$ ]. ....	40
Figure 15. Time Development of Semimajor Axis for a $M_{Jup}$ Size Planet about a $M_{sun}$ Central Star [ $B_o$ $= 5$ kG; $e = 0.0$ ; $\eta = 0.1$ ; $a_o = 0.04$ AU]. ....	42
Figure 16. Time Development of Semimajor Axis for a $M_{Jup}$ Size Planet about a $M_{sun}$ Central Star [ $B_o$ $= 5$ kG; $e = 0.0$ ; $\gamma = 1$ ; $a_o = 0.04$ AU]. ....	43
Figure 17. Time Development of Semimajor Axis for a $M_{Jup}$ Size Planet about a $M_{sun}$ Central Star [ $B_o$ $= 5$ kG; $a_o = 0.04$ AU; $\gamma = 1.0$ ; $\eta = 0.1$ ]. ....	45
Figure 18. Time Development of Semimajor Axis for a $M_{Jup}$ Size Planet about a $M_{sun}$ Central Star [ $e$ $= 0.0$ ; $\gamma = 1.0$ ; $\eta = 0.1$ ; $a_o = 0.04$ AU]. ....	46
Figure 19. Time Development of Semimajor Axis of a $M_{Jup}$ Size Planet about a $M_{sun}$ Central Star for Varying Initial Semimajor Axis Positions [ $e = 0.0$ ; $\gamma = 1.0$ ; $\eta = 0.1$ ; $B_o = 5$ kG]. ....	48

# I. Introduction

Over the past 11 years, since the discovery of the extrasolar planet 51 Pegasi b, just under 190 candidate extrasolar planets have been found among surveys of nearby FGKM stars. Through observational methods of Doppler radial velocity surveys, microlensing, and imaging, all but twelve candidates have been discovered using Doppler measurements. The findings have indicated that multiple planet systems are not uncommon and in fact often reside in resonant orbits. The largest extrasolar planet found to date is 17.4 Jupiter masses ( $M_{Jup}$ ) while the smallest planet is only a mere 5.5 Earth masses.

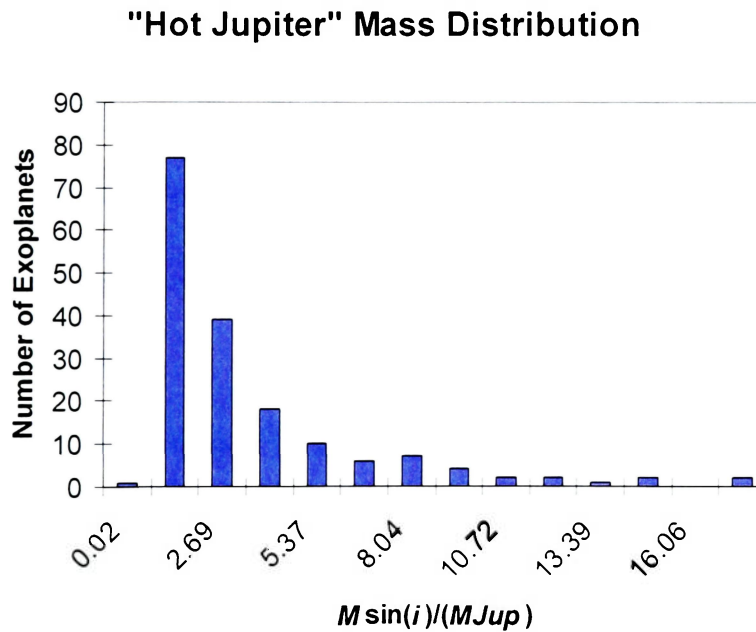
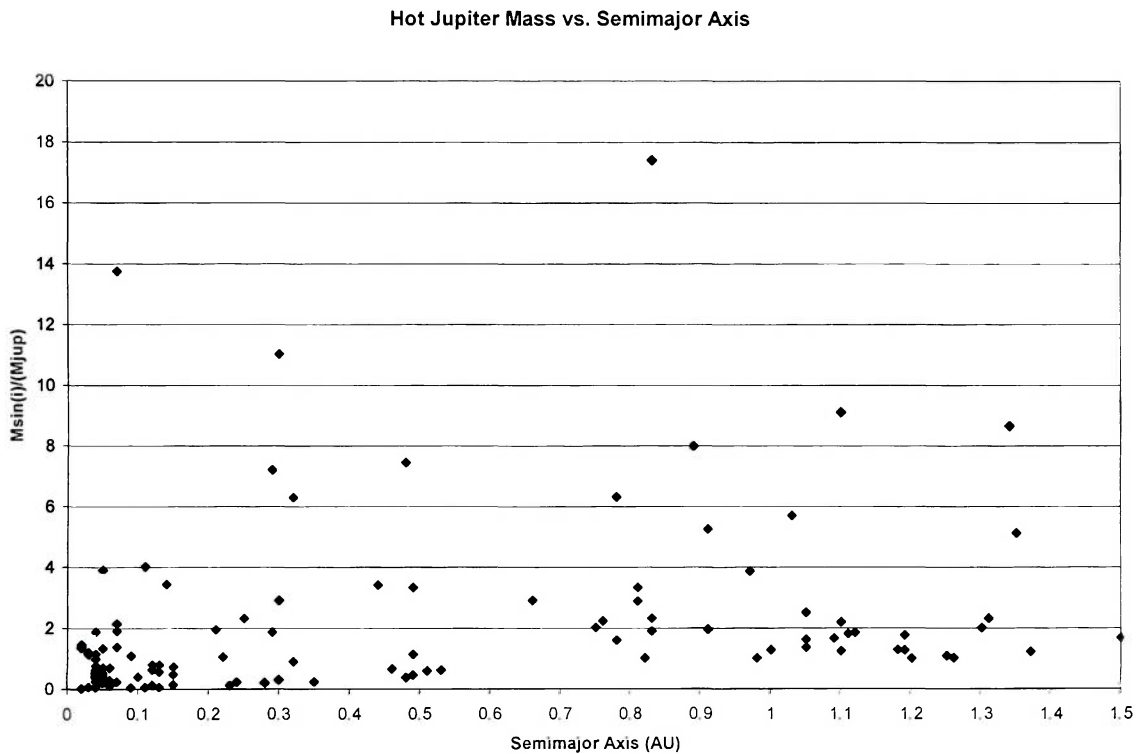


Figure 1. Extrasolar Planet  $M \sin(i) / M_{Jup}$  Histogram.

The mass distribution of planets has a strong tendency toward smaller masses. As can be seen in Figure 1 (Schneider 2006), there is a power law trend that approximates the shape of the curve for planetary mass distribution. Figure 2 (Schneider 2006) shows the distribution of planet mass with respect to semimajor axis for the close-in planets. Aside from a few outsiders, almost all the planets have small mass, with the majority below  $\sim 4M_{Jup}$ . Since there exists an observational bias toward large mass planets close in, it is surprising that the majority of them are low mass.



**Figure 2. Distribution of Extrasolar Planet  $M\sin(i)/M_{Jup}$  with Respect to Semimajor Axis (AU).**

Figure 3 (Schneider 2006) shows an unaccounted for “pile-up” of planets at extremely small orbital distances,  $a$ , approximately 0.04 AU, corresponding to an approximate 3-day orbital period. The reason that so many gas giant planets are located

at such close distances is yet to be explained. However, it is highly unlikely that these short-period gas giant planets, also known as “hot Jupiters”, formed at their present locations of  $a < 0.1$  AU. Rather, they most likely formed at much larger orbital distances and migrated inward through interactions with the remnants of the circumstellar planet-forming disk (Lin et al. 1996). The standard core accretion models for planet formation imagine small particles of ice and rock in the disk coagulating and accreting until they form a core of approximately 15 Earth masses. Gas, mainly composed of H and He is accreted from the disk and built up around the core of the planet. At the location of the hot Jupiters, ( $\sim 0.04$  AU), the temperature is approximately 2000 K. This is much too hot for small solid particles to exist (Lin et al. 1996). In addition to the previous problem with *in situ* gas giant planet formation, during the early stages of planet formation the radii are about ten times the current value; therefore, the escape speed from the planet would be much less allowing evaporation mechanisms and blow off from stellar wind to prevent formation.

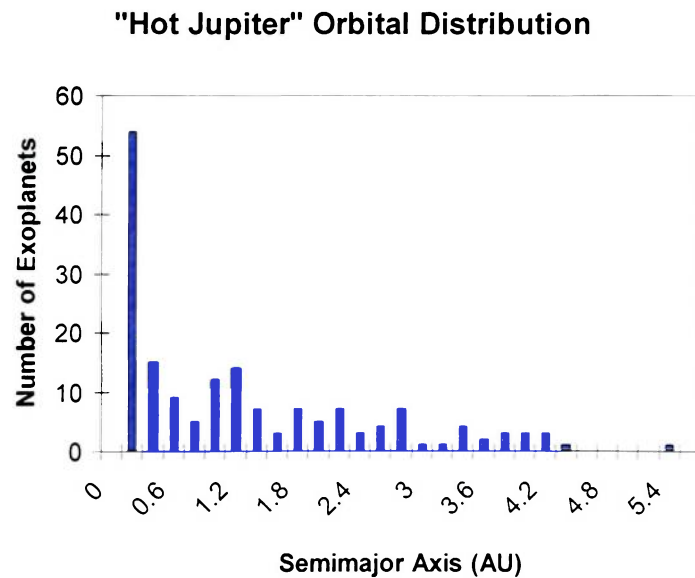


**Figure 3. Extrasolar Planet Semimajor Axis Histogram in AU.**

Three types of planet migrations are considered for giant planets. In Type I migration, a planet migrates inward too rapidly and loses all of its mass from a Roche lobe overflow. In Type II migration, a planet migrates inward, losing some mass, but stabilizing at a small heliocentric distance. Finally, in Type III migration, a planet does not lose any mass, typically not migrating very far at all from its formation location (Trilling et al. 1998). It is expected that when a planet has accreted a sufficient amount of mass, it will form a gap in the disk (Nelson & Papaloizou 2004). This is the beginning stage of planet migration. As the planet migrates inward, so does the gap. The planet will tidally interact with the disk resulting in an angular momentum transfer between the two (Trilling et al. 1998). The planet will start to clear material out of the disk from its orbit as density waves excite both interior and exterior to the planet from the tidal motion (See Figure 4). The gap in the disk depends on the mass of the planet and inversely with the viscosity of the disk (Lin & Papaloizou 1986).

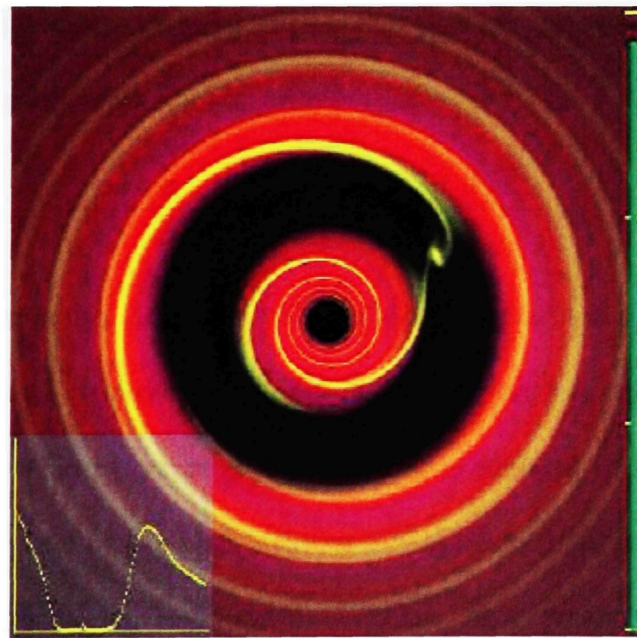


**Figure 4. Type II Gap Forming Planet Migration (Armitage & Rice 2005).**

Possible mechanisms for halting the inward migration of the hot Jupiters include Roche radius limits and tidal torque interactions. If a planet gets sufficiently close to its central star due to disk interactions, the planet's radius may exceed the Roche radius. If this happens, mass transfer from the planet to the star will occur. When this happens, the planet will migrate back out to conserve the angular momentum of the system. Once the planet's radius equals the Roche radius, mass transfer will cease. This means that its halting position is dependant on its own radius, therefore its own properties; temperature, age, and mass, etc.

Alternatively, tidal torques between the central star and the migrating planet may eventually halt the migration. During the T-Tauri evolutionary period of the central star, it will be rotating faster than the orbital period of the planet. As the planet approaches the star, tidal bulges will be raised on the star by the planet; however, they will not be aligned with the planet due to the star's rapid rotation. The planet will then slow the rotation of the star and move outward to conserve angular momentum. The radial motion of the planet due to the spin torque interaction with the star is given by

$$\frac{da}{dt} = \frac{9}{2} \Omega_p \frac{M_p}{M_{st}} \left( \frac{R_{st}}{a} \right)^4 \frac{R_{st}}{Q_{st}} \quad (1)$$

where  $R_{st}$  is the stellar radius,  $M_{st}$  is the stellar Mass,  $Q_{st}$  is the tidal dissipation factor of the star,  $M_p$  is the planetary mass, and  $\Omega_p$  is the Keplerian angular velocity of the planet (Trilling et. al. 1998). The value for  $Q_{st}$  represents how efficiently rotational energy is dissipated by friction within an object; its value is highly uncertain due to a lack of understanding of the details of the dissipation process. An estimated  $Q_{st} = 1.5 \times 10^5$  has been used for main-sequence stars (Lin et al. 1996); however, it ranges from  $1.5 \times 10^4 - 1.5 \times 10^6$  (Trilling et al. 1998). This estimate is based on the observation that the orbits

of short-period pre-main-sequence binary stars and main-sequence binary stars in the Pleiades cluster are circularized for periods less than about 5 and 7 days (Lin et al. 1996). The margin for error of this highly uncertain quantity, and therefore its influence on the semimajor axis of the hot Jupiter, is large enough to seriously doubt the ability of the tidal torques to halt a planet's inward migration. In any case, the tidal torque is effective while the star remains a rapid rotator, essentially losing its influence after  $10^8$  years (Skumanich 1972). In addition, the condition that tidal torques be responsible for the final location of a hot Jupiter requires that it take place before the star contracts substantially ( $< 10^7$  years), requiring a relatively small timeframe for this method to precisely halt the planet at observed heliocentric distances.

A potential mechanism proposed in this thesis for halting (and reversing) the inward migration, leading to the observed “pile up” of hot Jupiters at close distances to the central star, is the magnetic coupling between the planet and the protostar, with the resulting torque transferring angular momentum from the star to the planet. Approximating the magnetic field of the central star as a dipole field, the z-component is given by

$$B_z(a) = B_o \left( \frac{R_{st}}{a} \right)^3 \quad (2)$$

where  $B_o$  is the surface magnetic field. Magnetic torques can transfer angular momentum only if the Alfvén velocity is greater than the planet's orbital velocity. The Alfvén velocity is dependant upon the local magnetic field and gas density,  $\rho$ .

$$v_A = \frac{B_z}{\sqrt{4\pi\rho}}, \quad (3)$$

whereas, the orbital, or Keplerian velocity, depends on the central star's mass and the orbital distance of the planet:

$$v_k = \sqrt{\frac{GM_{st}}{a}}, \quad (4)$$

where  $G$  is the universal gravitational constant of  $6.67 \times 10^{-8} \text{ dyn cm}^2 \text{ g}^{-2}$ . Evaluating the inequality  $v_A \geq v_k$  to determine what range of semimajor axis that co-rotation can exist as well as using the dipole field approximation will determine if the magnetic field can provide a feasible torque to affect the planet's migration process. Inserting the dipole field into the Alfvén velocity expression and squaring both sides of the inequality produces

$$\frac{B_o^2 \left(\frac{R_{st}}{a}\right)^6}{4\pi\rho} \geq \frac{GM_{st}}{a}, \quad (5)$$

Solving the inequality for  $a$  yields

$$a \leq \left(\frac{B_o^2 R_{st}^6}{4\pi\rho GM_{st}}\right)^{1/5}. \quad (6)$$

Writing the stellar parameters in terms of solar system units, as well as referencing the surface magnetic field in typical T-Tauri magnitudes, this expression can be easily evaluated. Taking  $B_o$  to be a multiple of 5 kG (Matt & Pudritz 2005),  $M_{st}$  a multiple of  $M_{sun}$  (mass of the Sun,  $M_{sun} = 1.989 \times 10^{33} \text{ g}$ ),  $R_{st}$  a multiple of 2 times the solar radius ( $R_{sun} = 6.96 \times 10^{10} \text{ cm}$ ), and the density as a fraction of  $10^{-24} \text{ g cm}^{-3}$ , the semimajor axis in astronomical units,  $1 \text{ AU} = 1.49 \times 10^{13} \text{ cm}$ , is approximately



$$a_{AU} \leq 11 \frac{\left(\frac{B_o}{5kG}\right)^{2/5} \left(\frac{R_{st}}{2R_{sun}}\right)^{6/5}}{\left(\frac{\rho}{10^{-24} \text{ g/cm}^3}\right)^{1/5} \left(\frac{M_{st}}{M_{sun}}\right)^{1/5}}. \quad (7)$$

Since a hot Jupiter is defined as located at a distance of less than 0.1 AU from the central star, there exists a very large parameter space for the above condition to be met; especially considering that these planets are thought to form at distances of only  $\sim 5$  AU and then migrate in (Lin et al. 1996).

The efficiency of magnetic torques in halting planet migration can be estimated using the results of Lüst & Schlüter (1955) who found that for an infinitesimal flux-tube of cross-sectional area  $A$ , the transport of angular momentum,  $L$ , along the tube yields a torque

$$\tau_m = -\frac{aB_t B_p A}{4\pi}, \quad (8)$$

where  $B_t$  is the toroidal ( $\varphi$ ) and  $B_p$  is the poloidal ( $r$  and  $z$ ) components of the protostar's magnetic field. An approximate timescale for which the magnetic torque could influence the gas giant enough to locate it at  $\sim 0.04$  AU can be found by  $t \sim L/\tau$ .

Hoyle (1960) has estimated the original angular momentum of the planetary material in the Solar System to be  $\sim 4 \times 10^{51} \text{ g cm}^2 \text{ s}^{-1}$ . This value can be used as an upper limit of the total angular momentum that could be transferred into the hot Jupiter's orbital motion. As will be addressed in §III below, the toroidal and poloidal magnetic field strengths should be approximately equal. With  $B_o$  again in the 5 kG range,  $R_{st}$  to be some multiple of  $2R_{sun}$ , and making all conversions from the cgs-unit system to obtain  $t$  in years; the relationship in equation 9 is reached.

$$t_{yr} \approx 2.6 \times 10^{14} \left( \frac{(a/AU)^5}{\left( \frac{B_o}{5kG} \right)^2 \left( \frac{R_{st}}{2R_{sun}} \right)^8} \right) \quad (9)$$

Provided  $B_o = 5 \text{ kG}$ ,  $R_{st} = 2R_{sun}$ , and  $a = 0.04 \text{ AU}$ , the time taken for the planet to obtain that specified orbital distance is approximately  $10^6$  years. The rough estimate of this timescale coincides nicely with the timeframe necessary for planet formation and migration, and for the star to still be a rapid rotator and not have collapsed. The following sections will evaluate this torque in much more detail, considering the limitations and probable ranges of influence in which the magnetic torque will affect a planet. The time-dependent contraction of the central star's radius will be calculated and then applied toward the dipole field model in §II. An evaluation of the poloidal to toroidal magnetic component strengths will be addressed and then tested in §III and §VIC respectively. The semimajor axis derivation and results will be presented at the end of the document, §V and §VI, accompanied by plots demonstrating the effect on the strength of the torque for each contributing free parameter in the semimajor axis expression.

## II. Stellar Radius Size

For a dipole magnetic field, which is being used to model the stellar magnetic field, the field strength depends on the distance out from the star as well as the central star's radius (cf. equation 2). Thus, in order to consider the long-term affects of the magnetic coupling, allowance needs to be made for the contraction of the pre-main-sequence stars over a period of a million years or so. Using a combination of observational data and numerical calculations, this section will obtain a function for the stellar radius of a pre-main-sequence star with mass of order one a solar mass.

### A. *Parameters for Model Calculation*

D'Antona & Mazzitelli (1994) model the pre-main-sequence star contraction for Population I stellar structures of  $M_{st} < 2.5M_{sun}$ . Two models are tested for different over adiabatic convection models; the mixing-length theory [MLT] and the recent Cauto & Mazzitelli [CM] model. The nuclear network includes the complete  $p$ - $p$  chain and the CNO cycle while D and  ${}^7\text{Li}$  burning are considered separate since they are only relevant before the  $p$ - $p$  chain takes over. The optical atmosphere is limited to being "gray" using an expression for temperature as a function of opacity,  $T(\tau)$ , from Henyey, Vardya, & Bodenheimer (1965). Another two models are worked into the code using two separate radiative opacity values (Alexander et al.'s 1989 and Kurucz 1991) providing a total of four models for stellar luminosity,  $L$ , and effective temperature,  $T_{eff}$ , as functions of time.

The results of the four models showed that the MLT convection theory, when extended from the solar model to other evolutionary phases, did not provide results that were predictive in any way. Therefore, the only two models that were considered in the present study were the two models that used the CM convection model. Table 1 provides the data using the combination of the CM convection model with the Alexander radiative opacity values, while Table 2 provides the data which combines the CM convection model with Kurucz radiative opacity values (D'Antona & Mazzitelli 1994). Each was independently used to model the stellar radius of a pre-main-sequence central star with respect to its contraction in time.

**Table 1. Pre-Main-Sequence Stellar Properties Modeled Using the CM Convection Model in Conjunction with Alexander's (1989) Radiative Opacity Values (D'Antona & Mazzitelli 1994).**

Age (yr)	$M = 2M_{sun}$		$M = 1.5M_{sun}$		$M = 1M_{sun}$		$M = 0.5M_{sun}$	
	$Log L/L_{sun}$	$Log T_{eff}$ (K)	$Log L/L_{sun}$	$Log T_{eff}$ (K)	$Log L/L_{sun}$	$Log T_{eff}$ (K)	$Log L/L_{sun}$	$Log T_{eff}$ (K)
$7 \times 10^4$	1.657	3.683	1.657	3.677	1.61	3.655	0.614	3.629
$1 \times 10^5$	1.552	3.688	1.552	3.679	1.125	3.666	0.563	3.629
$2 \times 10^5$	1.295	3.699	1.295	3.689	0.893	3.672	0.492	3.628
$3 \times 10^5$	1.162	3.704	1.162	3.693	0.733	3.674	0.339	3.625
$5 \times 10^5$	1.005	3.709	1.005	3.697	0.551	3.675	0.079	3.616
$7 \times 10^5$	0.908	3.712	0.908	3.698	0.438	3.675	-0.067	3.609
$1 \times 10^6$	0.810	3.714	0.810	3.700	0.319	3.673	-0.211	3.601
$2 \times 10^6$	0.671	3.723	0.671	3.701	0.090	3.666	-0.473	3.582
$3 \times 10^6$	0.683	3.737	0.683	3.705	-0.042	3.661	-0.598	3.576
$5 \times 10^6$	1.202	3.804	1.202	3.719	-0.193	3.655	-0.738	3.572
$7 \times 10^6$	1.132	3.913	1.132	3.742	-0.267	3.655	-0.827	3.572
$1 \times 10^7$	1.205	3.962	1.205	3.788	-0.307	3.663	-0.921	3.572
$2 \times 10^7$	1.204	3.963	1.204	3.854	-0.169	3.718	-1.105	3.572
$3 \times 10^7$	1.205	3.963	1.205	3.855	-0.038	3.762	-1.206	3.573
$5 \times 10^7$	1.208	3.963	1.208	3.856	-0.156	3.754	-1.314	3.576
$7 \times 10^7$	1.212	3.962	1.212	3.856	-0.150	3.755	-1.360	3.580
$1 \times 10^8$	1.217	3.961	1.217	3.857	-0.145	3.755	-1.384	3.584

**Table 2. Pre-Main-Sequence Stellar Properties Modeled Using the CM Convection Model in Conjunction with Kurucz (1991) Radiative Opacity Values (D'Antona & Mazzitelli 1994)**

Age (yr)	$M = 2M_{sun}$		$M = 1.5M_{sun}$		$M = 1M_{sun}$		$M = 0.5M_{sun}$	
	Log $L/L_{sun}$	Log $T_{eff}$ (K)	Log $L/L_{sun}$	Log $T_{eff}$ (K)	Log $L/L_{sun}$	Log $T_{eff}$ (K)	Log $L/L_{sun}$	Log $T_{eff}$ (K)
$7 \times 10^4$	1 653	3 680	1 449	3 673	1 151	3 662	0 602	3 624
$1 \times 10^5$	1 559	3 687	1 392	3 677	1 116	3 663	0 546	3 623
$2 \times 10^5$	1 288	3 695	1 114	3 684	0 885	3 667	0 474	3 621
$3 \times 10^5$	1 154	3 699	0 972	3 687	0 724	3 668	0 338	3 617
$5 \times 10^5$	0 995	3 703	0 806	3 689	0 541	3 669	0 063	3 605
$7 \times 10^5$	0 896	3 705	0 699	3 690	0 425	3 667	-0 094	3 595
$1 \times 10^6$	0 800	3 708	0 588	3 690	0 302	3 664	-0 243	3 584
$2 \times 10^6$	0 663	3 718	0 389	3 690	0 067	3 655	-0 458	3 578
$3 \times 10^6$	0 671	3 731	0 299	3 694	-0 068	3 648	-0 562	3 580
$5 \times 10^6$	1 168	3 788	0 263	3 709	-0 222	3 640	-0 695	3 582
$7 \times 10^6$	1 123	3 911	0 344	3 730	-0 300	3 639	-0 785	3 584
$1 \times 10^7$	1 205	3 962	0 719	3 776	-0 342	3 646	-0 883	3 585
$2 \times 10^7$	1 204	3 963	0 691	3 851	-0 218	3 700	-1 074	3 586
$3 \times 10^7$	1 205	3 963	0 678	3 853	-0 019	3 753	-1 180	3 587
$5 \times 10^7$	1 208	3 963	0 681	3 854	-0 167	3 748	-1 293	3 589
$7 \times 10^7$	1 212	3 962	0 682	3 854	-0 161	3 748	-1 344	3 591
$1 \times 10^8$	1 217	3 961	0 685	3 854	-0 156	3 749	-1 373	3 593

## B. Calculation of Stellar Radius

The logarithmic values in Table 1 and Table 2 can be converted to  $L_{st}$  and  $T_{eff}$  in order to use a luminosity balance to find the approximate stellar radius of the central star as a function of time.

$$R_{st} = \sqrt{\frac{L_{st}}{4\pi\sigma T_{eff}^4}} \quad (10)$$

where  $\sigma$  is the Stefan-Boltzman constant which has a value  $5.6696 \times 10^{-5} \text{ erg cm}^{-2} \text{ K}^{-4} \text{ s}^{-1}$ . The resulting radii calculations are displayed in Table 3 and the MatLAB code used to make the calculations is presented in Appendix 2. The values show that there is minimal difference between the two models; they are of the same order magnitude. Therefore, the first model using the combination of the CM convection and Alexander's (1989) radiative opacity will be used.

**Table 3. Calculated Stellar Radius Values for 17 Different Stages in its Pre-Main-Sequence Evolution. All values in  $R_{sun}$  units.**

Age (yr)	CM + Alexander Model				CM + Kurucz Model			
	$M = 2M_{sun}$	$M = 1.5M_{sun}$	$M = 1M_{sun}$	$M = 0.5M_{sun}$	$M = 2M_{sun}$	$M = 1.5M_{sun}$	$M = 1M_{sun}$	$M = 0.5M_{sun}$
	$R_{st}/R_{sun}$				$R_{st}/R_{sun}$			
$7 \times 10^4$	9.663	7.927	5.931	3.729	9.752	7.963	5.944	3.764
$1 \times 10^5$	8.367	7.254	5.664	3.516	8.474	7.321	5.683	3.545
$2 \times 10^5$	5.917	5.089	4.218	3.255	5.979	5.147	4.277	3.293
$3 \times 10^5$	4.961	4.252	3.476	2.768	5.030	4.311	3.537	2.868
$5 \times 10^5$	4.047	3.456	2.806	2.138	4.112	3.529	2.852	2.208
$7 \times 10^5$	3.569	3.045	2.464	1.867	3.636	3.105	2.518	1.930
$1 \times 10^6$	3.159	2.664	2.168	1.641	3.211	2.733	2.216	1.710
$2 \times 10^6$	2.582	2.114	1.720	1.325	2.619	2.173	1.762	1.373
$3 \times 10^6$	2.455	1.873	1.512	1.179	2.489	1.924	1.558	1.207
$5 \times 10^6$	3.278	1.687	1.306	1.022	3.393	1.722	1.354	1.026
$7 \times 10^6$	1.831	1.704	1.200	0.923	1.828	1.716	1.243	0.916
$1 \times 10^7$	1.589	2.168	1.104	0.828	1.589	2.138	1.147	0.815
$2 \times 10^7$	1.580	1.452	1.005	0.670	1.580	1.466	1.032	0.651
$3 \times 10^7$	1.582	1.431	0.954	0.594	1.581	1.431	1.016	0.574
$5 \times 10^7$	1.587	1.428	0.864	0.477	1.587	1.429	0.877	0.499
$7 \times 10^7$	1.602	1.429	0.866	0.481	1.602	1.431	0.883	0.466
$1 \times 10^8$	1.618	1.428	0.871	0.460	1.618	1.436	0.884	0.447

### C. Results

Cameron (1995) modeled the stellar radius of the sun in time dependent form until the age of  $10^6$  years. The results in this study for stellar radius of the four different mass stars were plotted and fitted to the power function provided by Cameron (1995) to best represent the evolution of the central star based on the mass, luminosity, and effective temperature of the star.

$$R_{st}(t) = \left[ \left( \frac{28\pi\sigma T_{sur}^4}{GM_{st}^2} \right) t + \frac{1}{R_o^3} \right]^{-1/3} \quad (11)$$

where  $T_{sur}$  is the surface temperature of the star taken to be 4600 K, (Trilling et al. 1998) and  $R_o$  is the initial radius of the star, adjusted to best fit the data points. Since the first data point lies at  $7 \times 10^4$  years, the quality of the fit for earlier phases of evolution are unknown, but in any case, are not relevant to the later stages of planet formation

considered here. Figure 5 demonstrates the stellar radii as a function of time as well as the eye-fit power curve for each case. The  $R_o$  fit for each mass is listed in the following table:

**Table 4. Parameter Fits for the Power Function Estimate for the Time-Dependant Stellar Radius Value.**

$M_{st}/M_{sun}$	$R_o/R_{sun}$
0.5	10
1.0	12
1.5	14
2.0	16

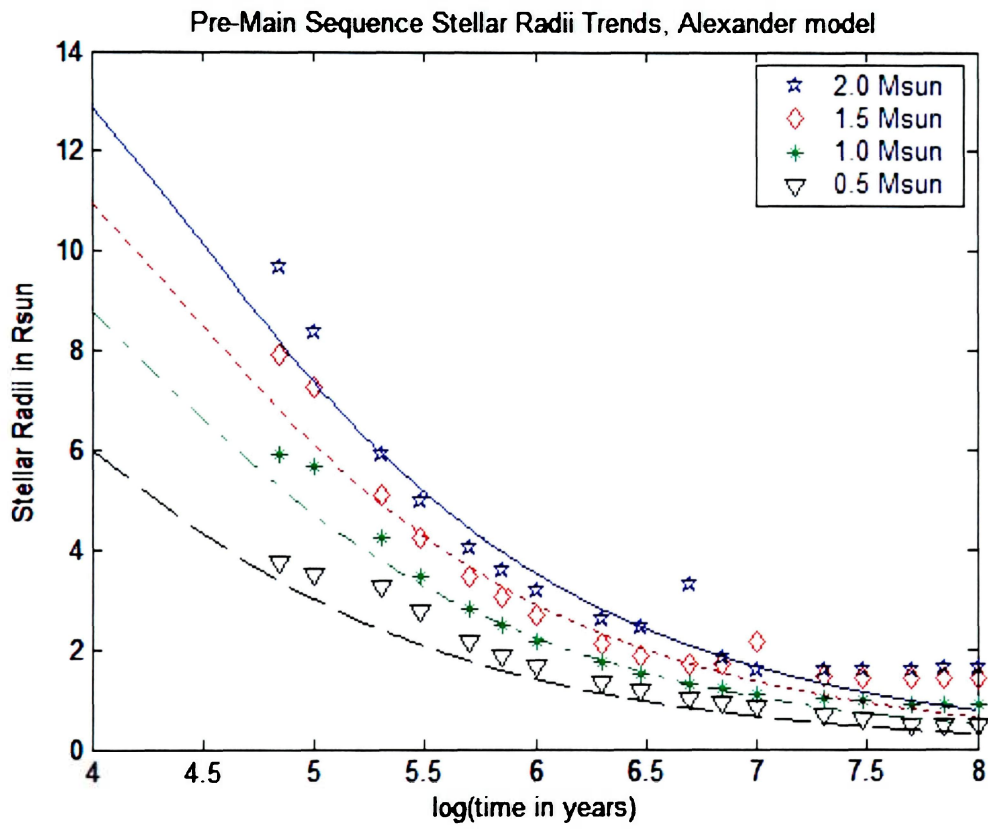


Figure 5. Stellar Radius Evolution for Different Sized Pre-Main-Sequence Stars. Best-fit Legend: solid- $2M_{sun}$ ; dotted- $1.5M_{sun}$ ; dash/dot- $1M_{sun}$ ; dashed- $0.5M_{sun}$ .



### III. Toroidal and Poloidal Magnetic Field Components

The magnetic torque received by the star, due to the presence of a gas giant planet passing through its magnetic field is given by equation 8:

$$\tau_m = -\frac{aB_t B_p A}{4\pi}. \quad (8)$$

The toroidal component of the central star's magnetic field is defined by the azimuthal,  $\varphi$ -component, of a typical cylindrical coordinate system. The poloidal component of the magnetic field depends on both the  $r$ - and  $z$ -components,  $B_p = \sqrt{B_r^2 + B_z^2}$ . Using the dipole field approximation provides a minimum for the strength of the magnetic torque because  $B_z \propto r^{-3}$  along the equator gives the weakest radial dependence of any natural magnetic field. Since the radial component,  $B_r$ , is negligible within the planet (Matt & Pudritz 2004), a free parameter  $\gamma = B_t/B_p$  will be defined as the ratio of the toroidal to poloidal magnetic fields in order to write the torque expression entirely in terms of the dipole field for the magnetic dependence.

The ratio of the magnetic fields,  $\gamma$ , represents the 'twist', or pitch angle, of the field. This is dependant on the physical coupling between the planet and the magnetic field lines of the star. In general, this coupling is not perfect. The magnetic forces act to resist the twisting of the field; they will attempt to 'slip' backward within the planet to try to straighten out. A few mechanisms can occur to make this physically happen; (1)

magnetic reconnection in the planet, (2) reconnection outside the planet, and (3) turbulent diffusion of the magnetic field through the planet (Matt & Pudritz 2005).

Although the coupling is not perfect, it is safe to assume there is a steady-state value of  $\gamma$ . If the slip-velocity were less (greater) than the speed of differential rotation between the planet and star,  $\gamma$  would increase (decrease) due to the twisting of the field lines on an orbital time-scale (Matt & Pudritz 2004). Thus, eventually, the slip-velocity will achieve a steady-state value equal to that of the differential rotation. If  $\gamma$  were to excessively exceed the critical field twist of  $\gamma_c \approx 1$  (when the critical differential rotation angle is  $\approx \pi$ ), the field lines will transition from a closed to open topology, therefore severing the magnetic connection between the planet and the star (Matt & Pudritz 2004).

Throughout the calculations  $\gamma$  will remain a variable; however, it has been shown it is safe to assume that the two field components will tend toward a steady-state of equal magnitudes ( $\gamma = 1$ ). As will be presented in §V, the dependence of the ‘twist’ is of order  $\gamma^{2/11}$  and is thus a rather insignificant parameter in the model.

## IV. Hot Jupiter Planetary Ionization

In order for the hot Jupiter to be able to couple to the magnetic field of the central star, the ion density within the planet needs to be high enough to “hold” onto the field lines. This will determine the efficiency of the ambipolar diffusion of the field lines through the planetary material. As shown in Figure 6, as the orbiting planet passes through the central star’s magnetic field, if the ion density is large enough, the ions of the planet will latch onto the field lines and will be essentially “frozen” to the field, exerting a torque on the star. During the early stages of planet formation, the gas giant planets are weakly magnetized so its own magnetic field will not act like a barrier in the same way Jupiter and Earth’s magnetospheres currently do (Penz et al. 2005). Only if the timescale for ambipolar diffusion is greater than the Keplerian orbital period of the planet, will the magnetic torque on the planet be significant. Ionization of a hot Jupiter is largely due to  $^{40}\text{K}$  and  $^{26}\text{Al}$  radioactivity, high energy X- and cosmic-rays, and ultraviolet radiation.

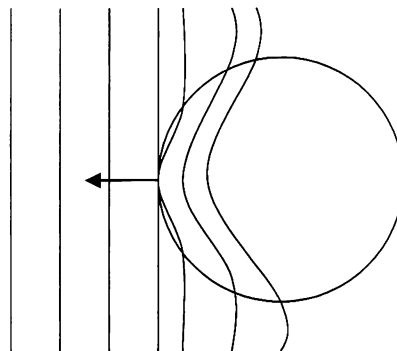


**Figure 6. Example of a Conductive Exoplanet Traveling Through the Magnetic Field Lines of the Central Star. If the Planet’s Resistivity is Low Enough, it will be “Frozen” to the Field Lines.**

### **A. Ionization by $^{40}\text{K}$ and $^{26}\text{Al}$ Radioactivity**

Potassium-40 is one of the most efficient ionization sources during planetary formation. Hydrogen is ionized by radioactivity in a gas giant planet. The rate at which ionization occurs is dependent on the abundance of radioactive elements. The half-life of potassium-40 is  $1.25 \times 10^9$  years. Correcting for the present meteoritic abundance of  $^{40}\text{K}$  backward to the time of solar system formation ( $4.5 \times 10^9$  years ago) and using this estimate as a good approximation for the abundance of  $^{40}\text{K}$  in other planetary systems during formation, there were  $4.35 \times 10^{-9}$   $^{40}\text{K}$  atoms per hydrogen atom (Nakano & Tademaru 1972). The ionization rate of hydrogen atoms for this abundance is (Nakano & Tademaru 1972)

$$\xi_K = 1.4 \times 10^{-21} \text{ s}^{-1}, \quad (12)$$

In addition to potassium-40, aluminum-26 is also a highly abundant and radioactive material capable of ionizing hydrogen atoms. The half life of  $^{26}\text{Al}$  is much shorter at only  $0.73 \times 10^6$  years. Positrons and  $\gamma$ -rays of energy 1.8 MeV are products of  $^{26}\text{Al}$  decay (Pudritz & Silk 1987). Pudritz & Silk (1987) estimate that the ionization rate of hydrogen atoms by  $^{26}\text{Al}$  can fall within the range stated in equation 13 for regions in which  $^{26}\text{Al}$  has not diffused (the low end) to ejections from Wolf-Rayet stars or high-density mediums (the high end)

$$10^{-22} \text{ s}^{-1} < \xi_{AL} < 10^{-19} \text{ s}^{-1}. \quad (13)$$

### **B. Ionization by X-rays**

Nakano & Tademaru (1972) estimate the background ionization rate by X-rays to be

$$\xi_x(\chi) = 1.9 \times 10^{-23} \chi^{-1.23} s^{-1}, \quad (14)$$

where  $\chi$  is the penetration depth from the surface of the planet ( $\text{g cm}^{-2}$ ) related to the actual depth,  $D$ , and density by  $\chi = \rho D$ . Ionization by X-rays with energy higher than 1 keV are effective, compared to the previously stated radioactivity, only when  $\chi < 0.03 \text{ g cm}^{-2}$ , thus X-ray ionization is not important at the high densities encountered in planets (Nakano & Tadamaru 1972).

### **C. Ionization by Cosmic Rays**

The cosmic-ray energy spectrum within a planet differs from that in interstellar space because the cosmic rays interact with matter (Nakano & Tadamaru 1972). The spectrum changes through energy losses by ionization, elastic  $p$ - $p$  scatterings, and pion-production collisions. The ionization rate of cosmic rays has been calculated by Nakano and Tadamaru (1972) to be

$$\xi_{CR}(\chi) = 6.1 \times 10^{-18} \exp\left(-\frac{\chi}{r}\right) s^{-1}, \quad (15)$$

where  $r = 66 \text{ g cm}^{-2}$  is the estimated mean range of cosmic rays in an interstellar gas cloud. The exponential factor deals with the loss of energy by the cosmic rays as they penetrate a medium and lose energy. This indicates that as the cosmic rays propagate through a highly dense medium, such as found in a planet, they will quickly lose energy, and the interior regions of the planet will effectively be shielded from this source of ionization.

### **D. Ionization by Ultraviolet Radiation**

Ultraviolet radiation is effectively screened by the grains and neutral atoms when the density of a medium reaches a value of  $n_H \sim 10^3 \text{ cm}^{-3}$  (Werner 1970). Therefore, the ionization from this source is significant only at very low densities. However, cosmic-ray ionization far exceeds ultraviolet ionization at low densities, so it is feasible to ignore ultraviolet radiation at all densities found in a planetary medium (Fleck & Hunter 1976). By excluding such sources of ionization, the ionization rate will be a lower limit. Therefore, any contributions from other sources will only strengthen the claim that a hot Jupiter is conductive enough to essentially be “frozen” to the magnetic field lines of the central star.

### ***E. Ion Density***

The ion density,  $n_i$ , for the interior of a giant gas planet can be calculated assuming equilibrium between ionization and recombination (Spitzer 1968). This assumes that the total rate at which ionization occurs,  $\zeta_{tot}$ , equals the rate of radiative recombination of electrons upon ions,  $R_e$  ( $\text{s}^{-1}$ ), and of electrons and ions upon the surfaces of dust grains,  $R_g$  ( $\text{s}^{-1}$ ). Zanstra (1954) determined the rate of radiative recombination of electrons and protons to be

$$R_e = 2.076 \times 10^{-11} n_e n_i T_{eff}^{-0.5} \phi(\beta), \quad (16)$$

where  $T_{eff}$  is the effective temperature of the planet,  $n_e$  and  $n_i$  are the densities of electrons and ions (protons) respectively, and  $\phi(\beta)$  is a function which changes with  $T_{eff}$ . The temperatures relevant for a hot Jupiter are in the  $(1 - 2) \times 10^3 \text{ K}$  range (Guillot et al. 1996) in which Zanstra (1954) uses a value of  $\phi(\beta) = 3.16$  for a temperature of 1580 K, a

value adopted here. In addition, it is assumed that  $n_e = n_i$ , so that equation 16 gives the relation  $R_e = 1.65 \times 10^{-12} n_i^2$ .

The radiative recombination rate of electrons and ions (protons) on the surface of grains is given by  $R_g = 2.21 \times 10^{-17} n_i$  (Nakano & Tademaru 1972). However, the temperature of a hot Jupiter may be strong enough to vaporize many grains (Elmegreen 1979), so this effect will be the weakest of the recombination methods. Equating the recombination rates with the minimum ionization rate provided by potassium-40 gives the minimum ion density ( $\text{cm}^{-3}$ ):

$$n_i = X(n_H \xi_K)^{0.5}, \quad (17)$$

where  $X$  is a constant that takes on a different value depending on the type of recombination which occurs.  $X$  has a minimum value of  $\sim 10^4$  for recombination on the surface of grains, a value of  $\sim 8 \times 10^5$  for radiative recombination, and an upper limit of  $\sim 3 \times 10^8$  for charge transfers (Oppenheimer & Dalgarno 1974 and Zanstra 1954).

## ***F. Ambipolar Diffusion***

Ambipolar diffusion is the drift of ions and electrons through a gas of neutral atoms (Spitzer 1968). The drift time is found from the magnetic field lines providing a driving force on the ions balancing the momentum exchange of collisions between primarily positive ions and neutral hydrogen atoms. The timescale for ambipolar diffusion is given by (Nakano & Tademaru 1972)

$$t_D = \frac{8\pi R_p^2 n_i n_H m_H \langle \sigma v \rangle}{B^2}, \quad (18)$$

where  $R_p$  is the planetary radius,  $m_H$  is the mass of a hydrogen atom (proton mass =  $1.67 \times 10^{-24}$  g) and  $\langle\sigma v\rangle$  is the product of the average collisional cross-section and velocity of the ions and atoms, which is dependant on the energy of the particles.

The ambipolar diffusion timescale needs to be greater than the Keplerian orbital period for the planet to have a high enough ion density to hold onto the field lines. The period of an orbiting planet is given by

$$P = \left( \frac{4\pi^2}{G} \right)^{1/2} \frac{a^{3/2}}{M_{st}^{1/2}} \quad (19)$$

Writing the density of neutral hydrogen atoms in terms of the overall planetary density,  $\rho = \mu m_H n_H$  (with an average molecular mass of  $\mu = 2$ ), substituting the ion density found in the previous section, and inserting the dipole magnetic field for the ambipolar diffusion timescales dependence on the semimajor axis of the planet provides and inequality  $t_D > P$  which can be solved for a limiting  $a$ . The required condition for the semimajor axis of the giant gas planet is

$$a > \frac{2^{2/9} \pi^{1/3} \mu^{1/3} m_H^{1/9} B_o^{4/9} R_{st}^{4/3} R_p^{5/9}}{G^{1/9} 3^{1/3} \langle\sigma v\rangle^{2/9} X^{2/9} \xi_K^{1/9} M_{st}^{1/9} M_p^{1/3}} \quad (20)$$

The only unknown in the above equation is the value for  $\langle\sigma v\rangle$ , the average product of the collision cross-section and velocity of the ions and atoms. This value is dependent on the energy of the particles, which can be found from the effective temperature,  $E = 3/2 k_B T_{eff}$  ( $k_B$  is the Boltzman constant,  $1.38 \times 10^{-16}$  erg K<sup>-1</sup>). Using the previously stated effective temperature of 1580 K, the energy per particle is  $3.27 \times 10^{-13}$  ergs or 0.2 eV. Shang et al. (2001) calculate the cross-section of a  $H^+ + H$  collision using a momentum transfer power law fit for a particle with energy greater than 0.01 eV to be



$$\sigma = 165 \times 10^{-16} \left( \frac{E}{0.01 \text{ eV}} \right)^{-1/8} \text{ cm}^2 \quad (21)$$

Evaluating the cross-section given  $E = 0.2 \text{ eV}$ , and using the kinetic energy to find the average velocity,  $E = 1/2 m_H v^2$ , the estimate for the product  $\langle \sigma v \rangle$  is  $7.1 \times 10^{-9} \text{ cm}^3 \text{ s}^{-1}$ . The extrasolar planet can be considered to be of order Jupiter-sized parameters; mass  $M_p = M_{Jup}$  and radii of order  $R_p = 10 R_{Jup}$ , where  $M_{Jup} = 1898.6 \times 10^{24} \text{ g}$  and  $R_{Jup} = 7.15 \times 10^9 \text{ cm}$  (Trilling et al. 1998). Once again, if the star's equatorial surface magnetic field  $B_o$  is taken to be in the 5 kG range,  $M_{st}$  to be approximately  $M_{sun}$ ,  $R_{st}$  to be  $2 R_{sun}$ , with the minimum sources of ionization and recombination considered,  $\xi = \xi_K$ , and  $X = 10^4$ , the semimajor axis requirement of a field-frozen gas giant planet (in AU) is given by

$$a_{AU} > 0.0136 \frac{\left( B_o / 5 \text{ kG} \right)^{4/9} \left( R_{st} / 2 R_{sun} \right)^{4/3} \left( R_p / 10 R_{Jup} \right)^{5/9}}{\left( \xi / \xi_K \right)^{1/9} \left( X / 10^4 \right)^{2/9} \left( M_{st} / M_{sun} \right)^{1/9} \left( M_p / M_{Jup} \right)^{1/3}}. \quad (22)$$

Since the minimum ionization was used in this calculation, any increase in either  $X$  or  $\xi$  will only decrease the necessary minimum semimajor axis distance, implying that all the hot Jupiter planets lie within a range of magnetic field influence. As shown in §I, the planet must be closer to the star than  $\sim 11 \text{ AU}$ . Here we see that the planet must be farther out than  $\sim 0.014 \text{ AU}$ , together providing the minimum parameter space for effective magnetic field coupling between an ionized gas giant planet and a dipole field from a pre-main-sequence central star. Within this range, the magnetic field will essentially be frozen to the planet and effective torques will exist.

## V. Semimajor Axis Calculation

The semimajor axis of an orbiting planet will depend on the angular momentum exchange it has between other bodies in the solar system. For the case considered here, there is one central star and one gas giant planet. The torque interaction between the two results from the magnetic coupling from the dipole magnetic field of the central star. A planet will either migrate in and speed up, or migrate out and slow down depending on the relationship between the planet's orbital velocity and the rotation rate of the central star. This section will calculate a planet's time-dependant semimajor axis due to angular momentum exchange with a central T-Tauri star that has a dipole magnetic field and radial evolution as described in §II.

### A. Torque Balance

Through the combination of Kepler's 2<sup>nd</sup> Law; an orbiting body has constant areal velocity, and Kepler's 3<sup>rd</sup> Law,  $\frac{P^2}{a^3} = \frac{4\pi^2}{G(M_{st} + M_p)}$ , the angular momentum of an orbiting planet of mass  $M_p$  and eccentricity  $e$  as a function of the changing semimajor axis can be found. The areal velocity,  $V$ , of an orbiting body about a focus with semimajor axis,  $a$ , and eccentricity  $e$ , is the total ellipse area over the orbital period:

$$V = \frac{\pi a^2 \sqrt{1-e^2}}{P}. \quad (23)$$

The angular momentum of the planet is the product of the linear momentum with the perpendicular radial component,  $L_p = mvy$  (refer to Figure 7). However, the product  $vy$  is twice the area of the triangle swept out per unit time to get from vertex  $C$  to vertex  $B$ , or, twice the areal velocity. Substituting equation 23 with Kepler's 3<sup>rd</sup> law written in terms of  $a$ , the angular momentum of an orbiting planet is given by

$$L_p = M_p \sqrt{G(1-e^2)(M_{st} + M_p)} a. \quad (24)$$

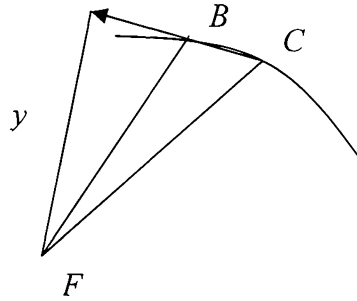


**Figure 7. The Picture shows the Area Swept Out by a Planet per Unit Time,  $BCF$ , and the Perpendicular Distance  $y$  from the Star to the Direction of Motion of the Planet.**

The torque on the orbiting body is found from differentiating its angular momentum with respect to time:

$$\tau_p = \frac{dL_p}{dt} = \frac{1}{2} M_p \sqrt{G(1-e^2)(M_{st} + M_p)} \frac{1}{\sqrt{a}} \frac{da}{dt}. \quad (25)$$

The exchange between the planet and the central star can be found by equating the magnetic torque on the star with the changing angular momentum of the planet.

$$\frac{dL_p}{dt} = - \frac{dL_{st}}{dt} \quad (26)$$

Substituting expressions 8 and 25 for the above exchange balance and using equations 2 and  $\gamma$  for the poloidal and toroidal field components, leads to

$$\frac{1}{2} M_p \sqrt{G(1-e^2)(M_{st} + M_p)} \frac{1}{\sqrt{a}} \frac{da}{dt} = \frac{\gamma B_o^2 R_{st}^6(t) A}{4\pi a^5} \quad (27)$$

The cross-sectional area,  $A$ , of the magnetic flux tube linking the planet to the central star can be taken to be some fraction,  $\eta$ , of the central star's top hemispherical area;  $A = \eta 4\pi R_{st}^2(t)$ . Making this substitution for  $A$ , and separating variables so that  $a$  is alone on the left-hand side of the equation, yields the following relationship:

$$a^{9/2} da = \frac{2\gamma\eta B_o^2 R_{st}^8(t)}{M_p \sqrt{G(1-e^2)(M_{st} + M_p)}} dt. \quad (28)$$

The most influential variable in this expression is the stellar radius, calculated in §II. The specific model provided expressions for the radial evolution for four specific stellar masses;  $2M_{sun}$ ,  $1.5M_{sun}$ ,  $1M_{sun}$ , and  $0.5M_{sun}$ . It should be noted that although the constants in Table 4 are different, the time-dependent radius functions all take the same form of  $R_{st}(t) = \left(c_1 t + \frac{1}{c_2}\right)^{-1/3}$ , where  $c_1 = \frac{28\pi\sigma T_{sur}^4}{GM_{st}^2}$  and  $c_2 = R_o^3$ . The generic form of stellar radius evolution can be substituted into the previous equation before integrating both sides to solve for the dependence of the semimajor axis of an orbiting planet on time:

$$\int_{a_o}^a a^{9/2} da' = \int_0^t \frac{2\gamma\eta B_o^2 \left(c_1 t' + \frac{1}{c_2}\right)^{-8/3}}{M_p \sqrt{G(1-e^2)(M_{st} + M_p)}} dt'. \quad (29)$$

The initial condition for this analysis begins at  $t = 0$ ; however, in addition to this assumption is an artificial initial condition which assumes that the planet has already formed and migrated inward some distance  $a_o$ . The effect of this constant on the final

location of the planet undergoing an outward torque from the star will be examined in

§VI. Evaluating the integrals leads to

$$\frac{2}{11} \left( a^{11/2}(t) - a_o^{11/2} \right) = \frac{2\gamma\eta B_o^2}{M_p \sqrt{G(1-e^2)(M_{st} + M_p)}} \frac{-3c_2^{5/3}}{5c_1(c_1c_2t'+1)^{5/3}} \Big|_0^t. \quad (30)$$

Taking the necessary algebraic steps leads to the final relationship of the semimajor axis of an orbiting planet with respect to time:

$$a_{cm}(t) = \left[ a_o^{11/2} + \frac{11}{2} \frac{6c_2^{5/3}\gamma\eta B_o^2}{5c_1M_p\sqrt{G(1-e^2)(M_{st} + M_p)}} \left( 1 - (c_1c_2t + 1)^{-5/3} \right) \right]^{2/11}. \quad (31)$$

The above expression is evaluated with the cgs-units system. In order to obtain the value in solar-system units, equation 31 needs to be divided by the number of

centimeters in an astronomical unit;  $a_{AU}(t) = \frac{a_{cm}(t)}{1.496 \times 10^{13} \text{ cm} / AU}$ . The results section

will explore the implications of all the parameters in equation 31. The semimajor axis depends on the fractional parameters  $\gamma$  and  $\eta$  as well as the stellar components  $B_o$ ,  $M_{st}$ ,  $c_1$ , and  $c_2$ , and the planetary properties  $M_p$ ,  $e$ , and  $a_o$ .

## **B. Angular Momentum Exchange**

A necessary condition that needs to be met in this model is that the star has enough angular momentum through rotation to push the planet outward. If this condition were not met, the star would not have the angular momentum to transfer. As the planet is pushed outward and settles into a steady-state location, the star eventually spins down from a rapid rotator in the T-Tauri phase to a slow rotator in the main-sequence phase of its life. The angular moment of the rotating star can be found by taking its moment of inertia to be some factor,  $f$ , of a near perfect sphere.

$$L_{st} = fM_{st}R_{st}^2\omega, \quad (32)$$

where  $\omega$  is the star's angular velocity.

Since a star is centrally condensed,  $f$  can be taken to be approximately 0.1 (compared to 0.4 for a uniform sphere). Herbits et al. (2002) monitored T-Tauri stars in the Orion Nebula Cluster for 45 nights and found a spread of angular velocities between 0.5 rad/d to 10 rad/d (above 2 rad/d qualifies the star as a rapid rotator). The majority of the stars had angular velocities between 2 rad/d and 4 rad/d; therefore, the angular velocity for a typical T-Tauri star,  $\omega_{TT}$ , will be taken to be  $\sim 3$  rad/d. The central stars are taken to be of order  $M_{sun}$  and  $2R_{sun}$ , which leads to an angular momentum value in cgs-units ( $\text{g cm}^2 \text{s}^{-1}$ ) of

$$L_{st} = 1.33 \times 10^{50} \left( \frac{f}{0.1} \right) \left( \frac{M_{st}}{M_{sun}} \right) \left( \frac{R_{st}}{2R_{sun}} \right)^2 \left( \frac{\omega}{\omega_{TT}} \right). \quad (33)$$

The magnitude of angular momentum that the planet has is dependent on the orbital parameters, such as the semimajor axis; if the semimajor axis increases, so does the angular momentum. As previously shown, however, taking the planet to be of order  $M_{Jup}$  and the semimajor axis to be in astronomical units, the expression for a planet orbiting at a distance  $a$  from its central star is given in cgs-units ( $\text{g cm}^2 \text{s}^{-1}$ ) by

$$L_p = 8.46 \times 10^{46} \left( \frac{M_p}{M_{Jup}} \right) \sqrt{(1 - e^2) \left( \frac{M_{st}}{M_{sun}} + 9.55 \times 10^{-7} \frac{M_p}{M_{Jup}} \right) \left( \frac{a}{AU} \right)}. \quad (34)$$

The important thing to consider as a planet transits from approximate 0.01 AU out to a few AU is that its gain in angular momentum does not exceed what the star has to offer. Table 5 provides a chart for the angular momentum calculation as a planet moves outward provided the planetary system properties of  $M_p = M_{Jup}$ ,  $M_{st} = M_{sun}$ , and  $e = 0.0$ .

**Table 5. Gain in Angular Momentum of an Orbiting Jupiter Sized Planet Around a Solar Mass as its Semimajor Axis Increase in 0.5 AU Step-Sizes**

$e = 0.0; M_p = M_{Jup}; M_{\star} = M_{sun}$	
$a$ (AU)	$L_p$ ( $\text{g cm}^2 \text{s}^{-1}$ )
0.01	$0.0846 \times 10^{47}$
0.51	$0.6040 \times 10^{47}$
1.01	$0.8500 \times 10^{47}$
1.51	$1.0394 \times 10^{47}$
2.01	$1.1992 \times 10^{47}$
2.51	$1.3400 \times 10^{47}$
3.01	$1.4674 \times 10^{47}$
3.51	$1.5846 \times 10^{47}$
4.01	$1.6938 \times 10^{47}$
4.51	$1.7963 \times 10^{47}$
5.01	$1.8932 \times 10^{47}$
5.51	$1.9854 \times 10^{47}$

It is seen from Table 5 that the gain in angular momentum of the planet as it drifts outward due to momentum transfer from the central star is less than the total angular momentum of a solar type T-Tauri star during its phase of rapid rotation. Therefore, it is possible for the star to have the ability to halt the inward migration.

## VI. Results

The time evolution of the semimajor axis of a planet orbiting a central star under the influence of a magnetic dipole field can now be calculated. The distribution of semimajor axis with respect to the various parameter inputs was solved in equation 31. Substituting the expressions for the constants  $c_1$  and  $c_2$  yields:

$$a_{cm}(t) = \left[ a_o^{11/2} + \frac{33\gamma\eta B_o^2 \sqrt{GM_{st}^2 R_o^5}}{140M_p (\pi\sigma T_{sur}^4) \sqrt{(1-e^2)(M_{st} + M_p)}} \left( 1 - \left( \frac{28\pi\sigma T_{sur}^4 R_o^3}{GM_{st}^2} t + 1 \right)^{-5/3} \right) \right]^{2/11} \quad (35)$$

As previously stated in §II,  $T_{sur}$  can be taken to be 4600 K (Trilling et al. 1998) and  $R_o$  is dependent on  $M_{st}$ .

### A. Central Star Mass

For a planet-star system of  $M_p = M_{Jup}$ ,  $e = 0.0$ ,  $B_o = 5$  kG,  $\gamma = 1.0$ , and  $\eta = 0.1$ , Figure 8, Figure 9, Figure 10, and Figure 11 show the semimajor axis progression (in AU) of the planet for decreasing stellar mass of  $2M_{sun}$ ,  $1.5M_{sun}$ ,  $M_{sun}$ , and  $0.5M_{sun}$  respectively. All plots evaluate the planet's orbital evolution for five different initial semimajor axis conditions;  $a_o = 0.01, 0.11, 0.21, 0.31,$  and  $0.41$  AU. The most noticeable trait among the four figures is that as the stellar mass decreases, the distance to which the planet is pushed out decreases as well. This is expected since the magnetic field strength is dependent on the size,  $R_{st}$ , of the star which is intrinsically dependent on the mass of the star. Every physical action that went into the solution found in equation 31 depends



on the mass of the star; the orbital angular momentum of the planet the dipole magnetic field, and flux tube cross-sectional area. Therefore, this parameter is expected to be the most influential variable in the strength of the magnetic torque.

As the star begins to contract, the strength of the magnetic torque declines and the planet settles into a steady state semimajor axis between  $\sim 0.32$  AU and  $\sim 0.57$  AU. Since the strengths of the *inward* migration have not been considered in this study, it is no surprise that these values are larger than the “hot Jupiter” definition of  $a < 0.1$  AU; the purpose here was only to demonstrate the efficiency of a magnetic torque in pushing planets *outward*. The final resting location of the planet depends more strongly on the stellar mass than it does on the initial semimajor axis, as can be seen from the figures. What is noticeable is that as the stellar mass increases, the deviation of final location weakens based on initial semimajor axis. It should be expected that there would be some distribution of end orbital distances based on initial position. The reason that the final orbital location has a wider range in the smaller mass stars versus the larger mass stars comes from the contraction phases of the star’s radius. Referring once again to Figure 5, one sees that although the initial radius variation is strong between the four different stellar masses, they all converge to a small range of final star size between  $0.5R_{sun}$  and less than  $2.0R_{sun}$ . Therefore, the larger mass stars have a very strong influence on a planet’s orbital radius during the early stages of migration, but weakens to a magnetic torque of similar strength to that of a smaller mass central star. This is the reasoning for the distribution of final semimajor axis to be smaller for the greater mass stars than for the smaller mass stars.

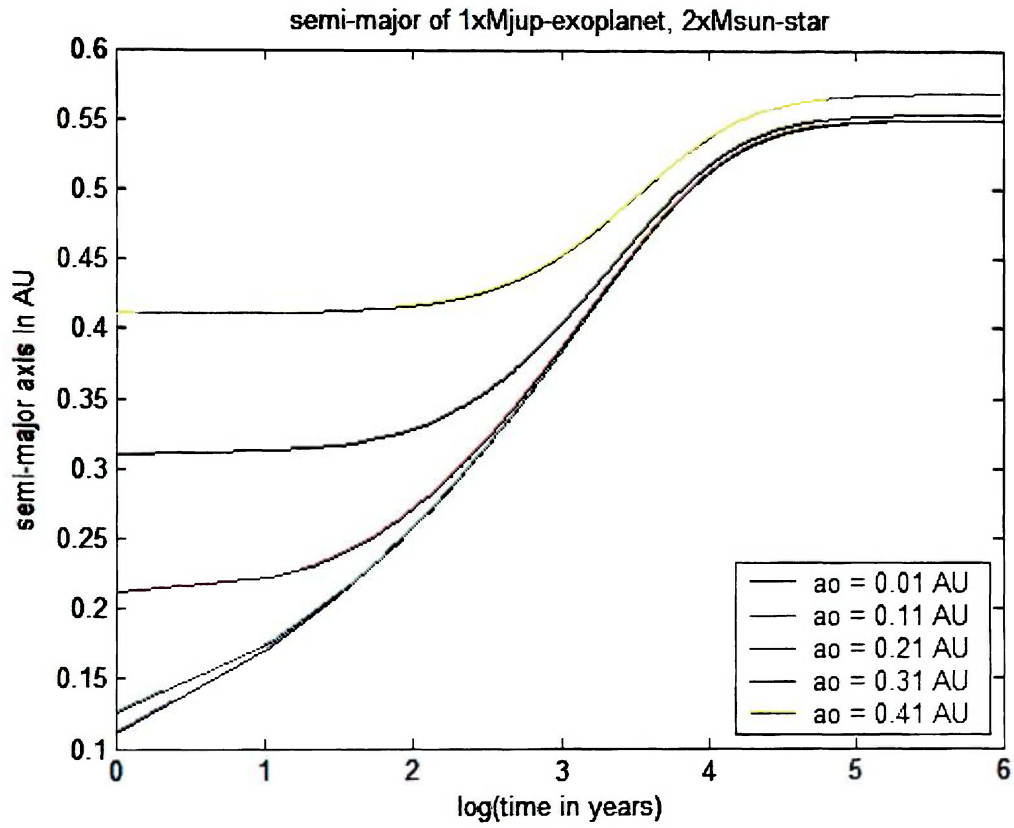


Figure 8. Time Development of Semimajor Axis for a  $M_{Jup}$  Size Planet about a  $2M_{sun}$  Central Star for Varying Initial Semimajor Axis Positions [ $B_o = 5$  kG;  $e = 0.0$ ;  $\gamma = 1$ ;  $\eta = 0.1$ ].

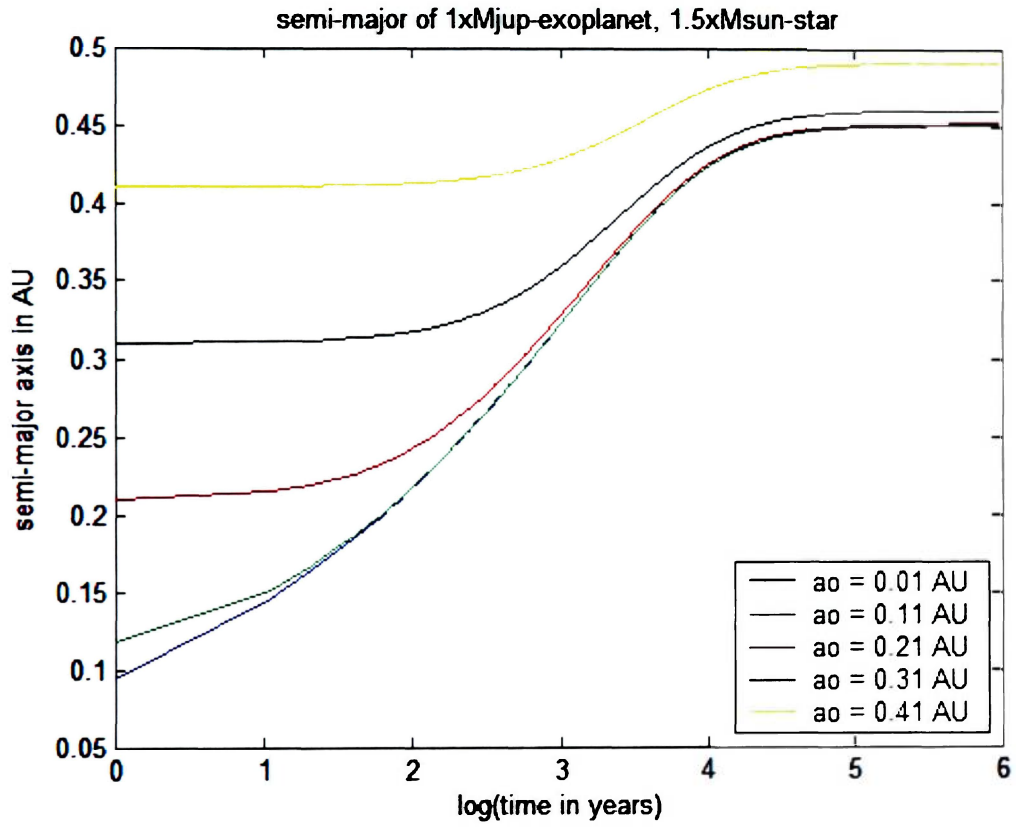


Figure 9. Time Development of Semimajor Axis for a  $M_{Jup}$  Size Planet about a  $1.5M_{sun}$  Central Star for Varying Initial Semimajor Axis Positions [ $B_o = 5$  kG;  $e = 0.0$ ;  $\gamma = 1$ ;  $\eta = 0.1$ ].

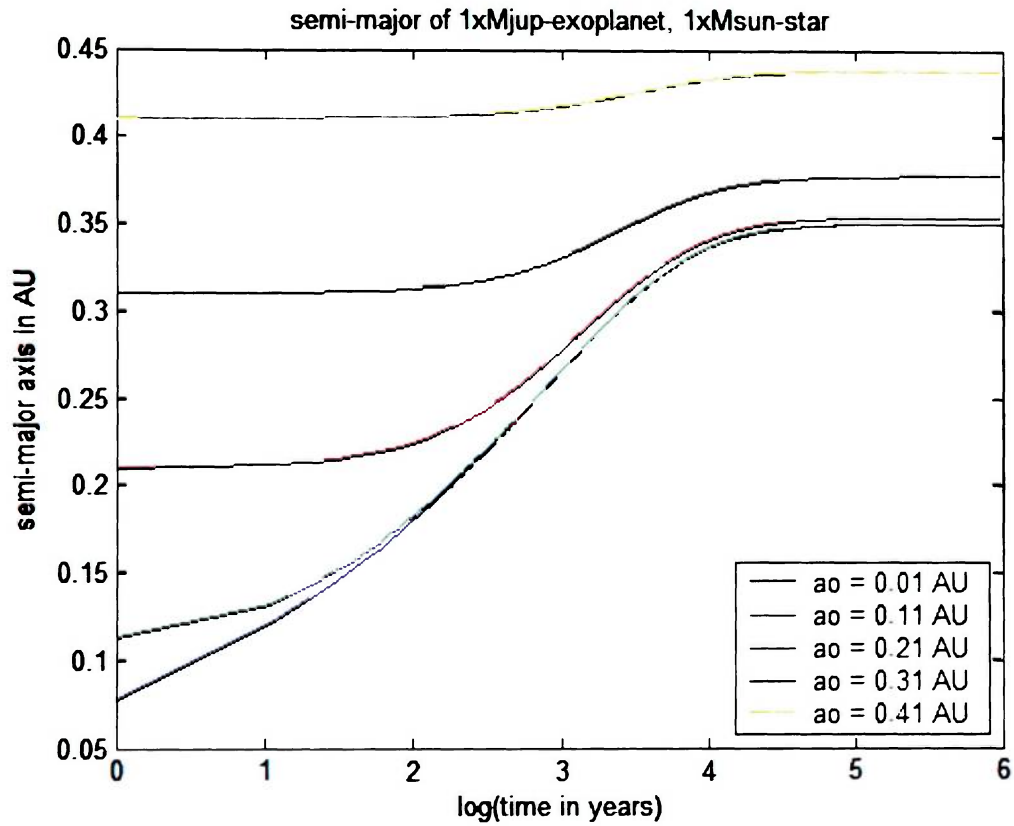


Figure 10. Time Development of Semimajor Axis for a  $M_{Jup}$  Size Planet about a  $M_{Sun}$  Central Star for Varying Initial Semimajor Axis Positions [ $B_o = 5$  kG;  $e = 0.0$ ;  $\gamma = 1$ ;  $\eta = 0.1$ ].

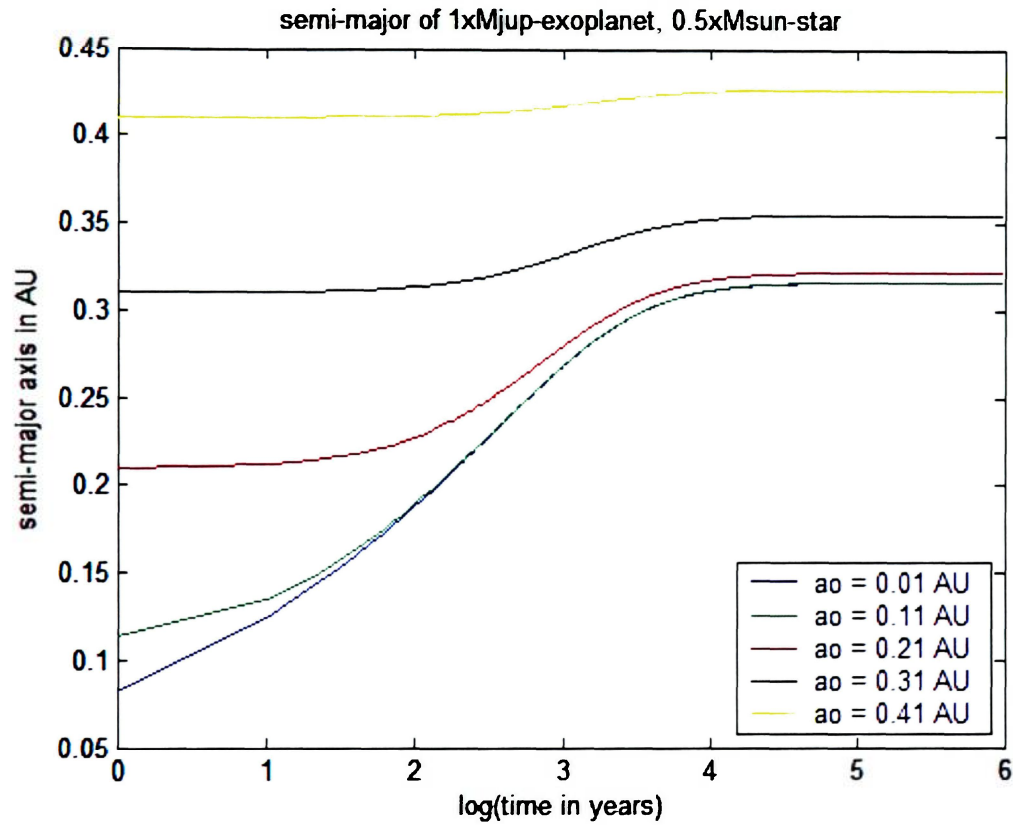


Figure 11. Time Development of Semimajor Axis for a  $M_{Jup}$  Size Planet about a  $0.5M_{sun}$  Central Star for Varying Initial Semimajor Axis Positions [ $B_o = 5$  kG;  $e = 0.0$ ;  $\gamma = 1$ ;  $\eta = 0.1$ ].

## B. Planet Mass

In much the same way that the variation in stellar mass was evaluated, the effect of planetary mass was calculated for the same range of initial semimajor axis  $a_o$  and other planet-star system parameters. The results are plotted in Figure 12 ( $M_p = 10M_{Jup}$ ), Figure 13 ( $M_p = 5M_{Jup}$ ), Figure 10 ( $M_p = 1M_{Jup}$ ), and Figure 14 ( $M_p = 0.1M_{Jup}$ ). As expected the influence of varying the planet's mass on the final semimajor axis magnitude is not as strong as varying the star's mass. The dependence on the planet's mass derives from the orbital angular momentum of the planet. The variable enters the equation through Kepler's 3<sup>rd</sup> Law, the dependence of the gravitational coupling for an orbiting body about a central mass. Since the planetary mass is so much smaller than the stellar mass, its influence on the gravitation pull of the system is minimal.

If the mass of the planet increases, it will be more difficult for the central star to push out the planet. This is shown in the figures; the final orbital location for the smallest mass planet is the largest. For the planets originating at 0.41 AU, there is a decent push on the  $0.1M_{Jup}$  planet out to almost 0.7 AU (see Figure 14); however, the largest planet,  $10M_{Jup}$ , doesn't really get pushed out at all (see Figure 12). Also, for the planets originating at 0.01 AU the push on the larger planet is only out to  $\sim 0.23$  AU and the smaller planet gets pushed out to  $\sim 0.68$  AU. In the same sense that it is easier for a star to hold off a small planet, it will be easier for the tidal interactions between the planet and the disk to push in a small planet; therefore, there may exist a balance between the opposing forces to group the planets in the hot Jupiter range.

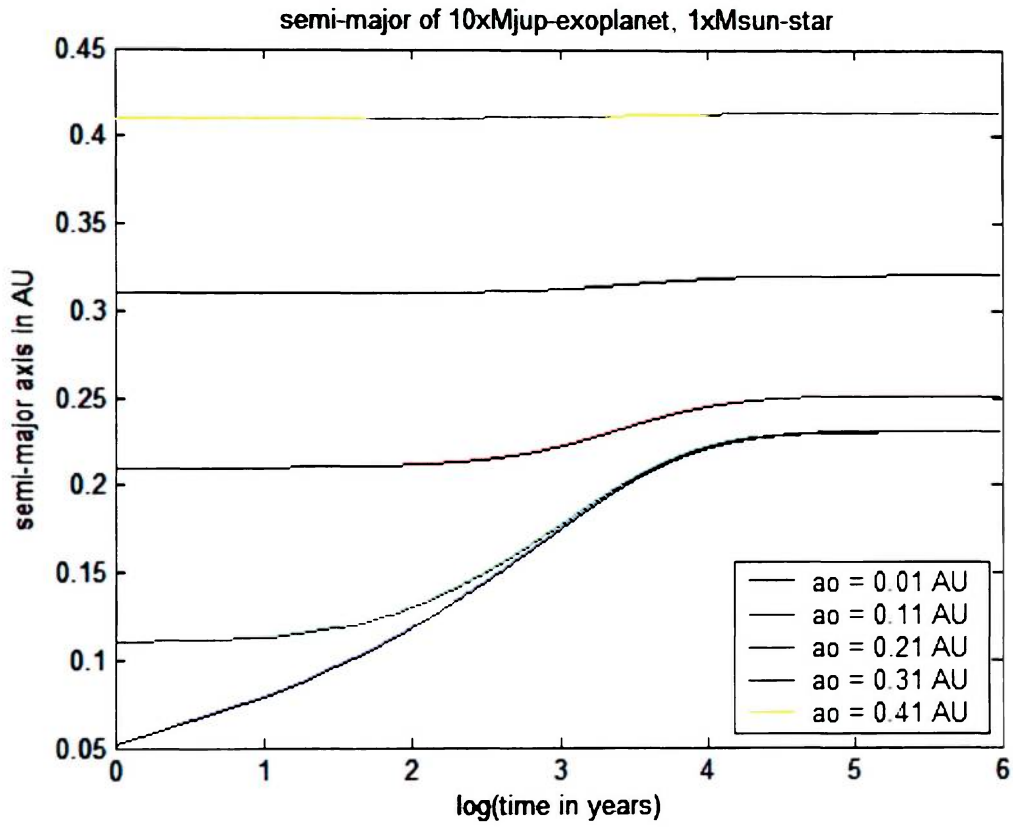


Figure 12. Time Development of Semimajor Axis for a  $10M_{Jup}$  Size Planet about a  $M_{sun}$  Central Star for Varying Initial Semimajor Axis Positions [ $B_o = 5$  kG;  $e = 0.0$ ;  $\gamma = 1$ ;  $\eta = 0.1$ ].

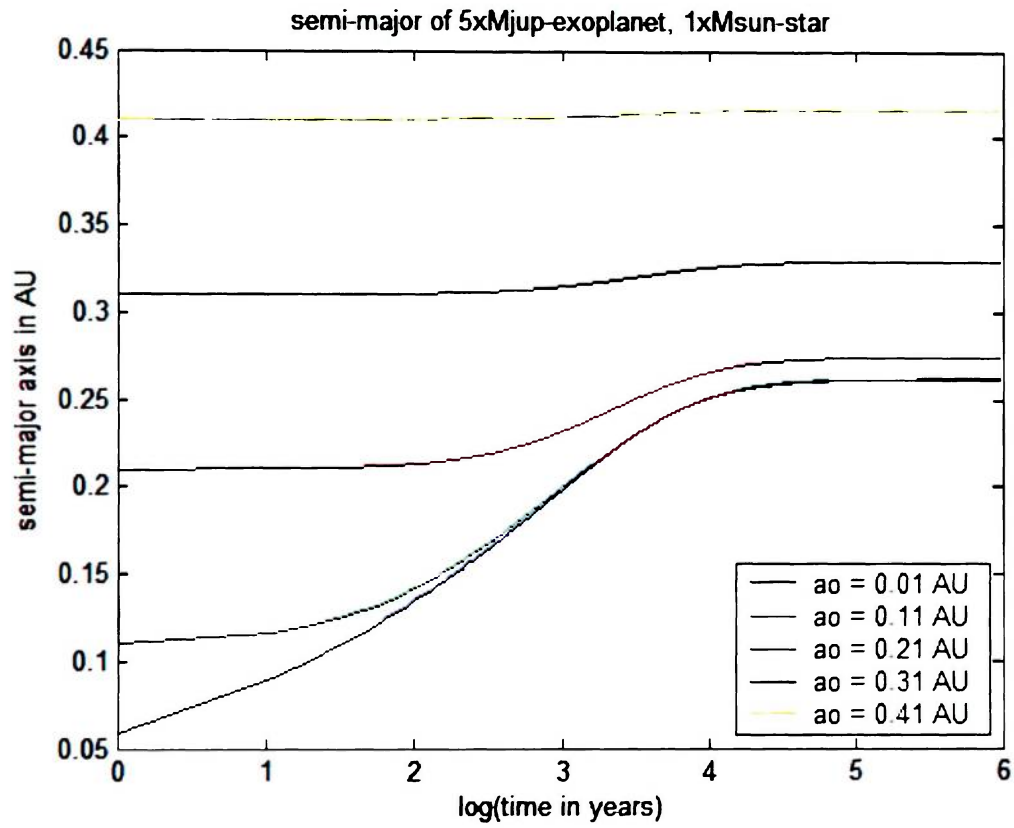


Figure 13. Time Development of Semimajor Axis for a  $5M_{Jup}$  Size Planet about a  $M_{sun}$  Central Star for Varying Initial Semimajor Axis Positions [ $B_o = 5$  kG;  $e = 0.0$ ;  $\gamma = 1$ ;  $\eta = 0.1$ ].



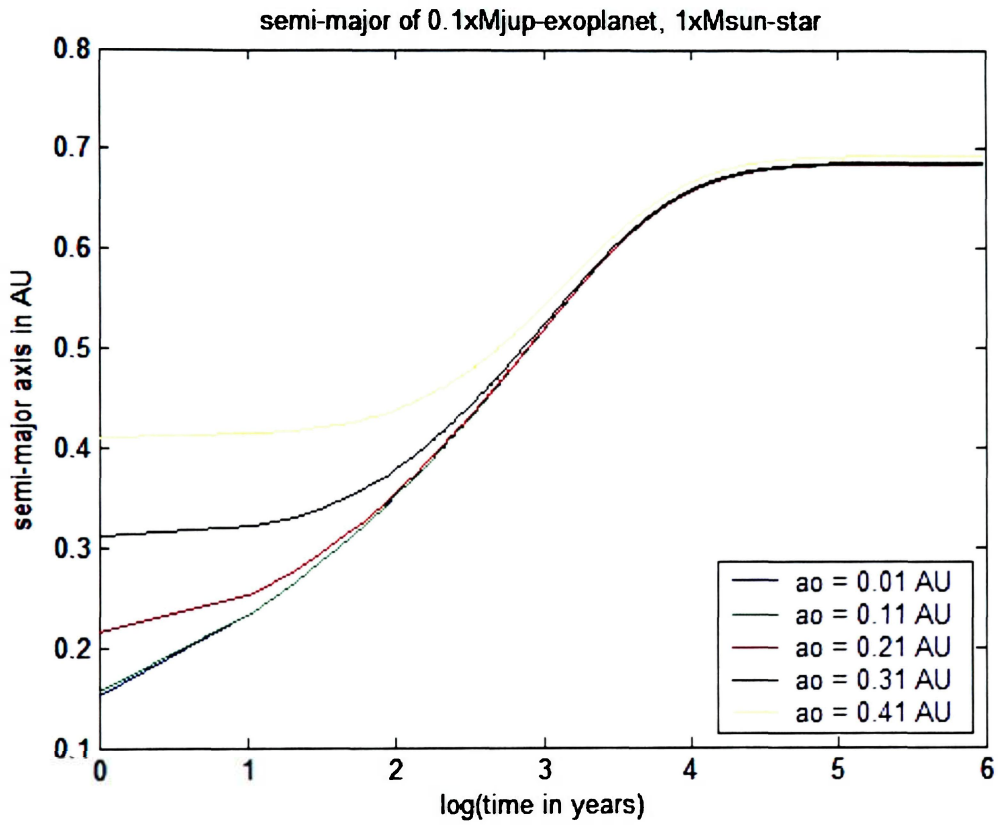


Figure 14. Time Development of Semimajor Axis for a  $0.1M_{Jup}$  Size Planet about a  $M_{sun}$  Central Star for Varying Initial Semimajor Axis Positions [ $B_o = 5$  kG;  $e = 0.0$ ;  $\gamma = 1$ ;  $\eta = 0.1$ ].

### **C. Ratio of Poloidal to Toroidal Magnetic Field Components and Magnetic Flux Tube Footprint**

The magnetic torque coupling between the central star and orbiting planet depend on the parameters  $\gamma$  and  $\eta$ ; however, in equation 31 they are raised only to the  $^{2/11}$  power so it is expected that these parameters have little influence over the semimajor axis of an orbiting planet. Figure 15 demonstrates the influence of the toroidal to poloidal magnetic field ratio  $\gamma$  for values between 0.1 to 2.0. In this planet-star system only one initial semimajor axis condition was used, that of the typical hot Jupiter location, 0.04 AU. In addition, the other parameters such as  $B_o = 5$  kG,  $\eta = 0.1$ ,  $e = 0.0$ ,  $M_p = M_{Jup}$ , and  $M_{st} = M_{sun}$  were used for the calculation. Figure 16 displays nearly the same calculation but instead  $\gamma$  is held constant at 1.0 and  $\eta$  is varied between 0.01 and 0.2.

The two Figures are nearly identical, indicating that these parameters have minimal influence over the final orbital location of the planet. Even though the two parameters are varied between much different ranges, their final results are the same. As is shown, the orbital distance does increase with increasing values for these parameters, so as expected, if the product of the magnetic field components or the magnetic flux tube area linking the star with a planet increase, the torque will be stronger. But it should be noted that the variation between final semimajor axis distributions for the toroidal to poloidal magnetic field component is only approximately  $\pm 0.1$  AU from the most likely case of  $\gamma = 1$  as justified in §III. The same holds true for the area of magnetic flux tube interception, which should be approximately 0.1 if the size of the planet to star is similar to that of Jupiter and the Sun.

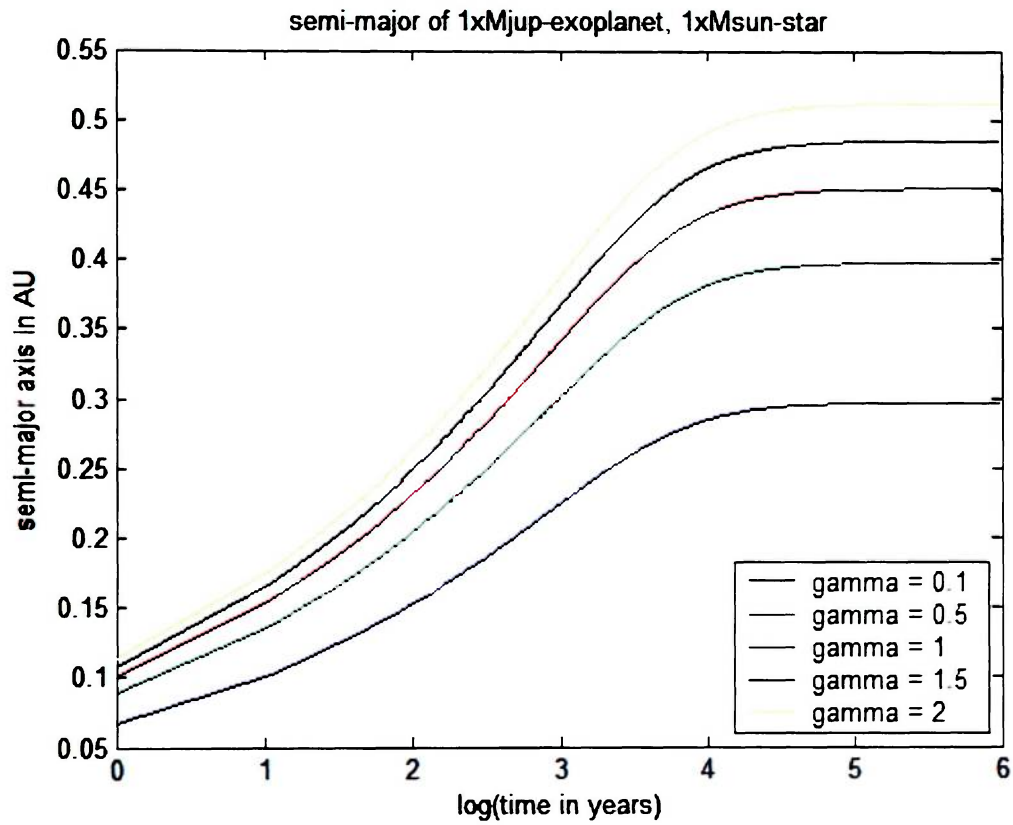


Figure 15. Time Development of Semimajor Axis for a  $M_{Jup}$  Size Planet about a  $M_{sun}$  Central Star [ $B_o = 5$  kG;  $e = 0.0$ ;  $\eta = 0.1$ ;  $a_o = 0.04$  AU].

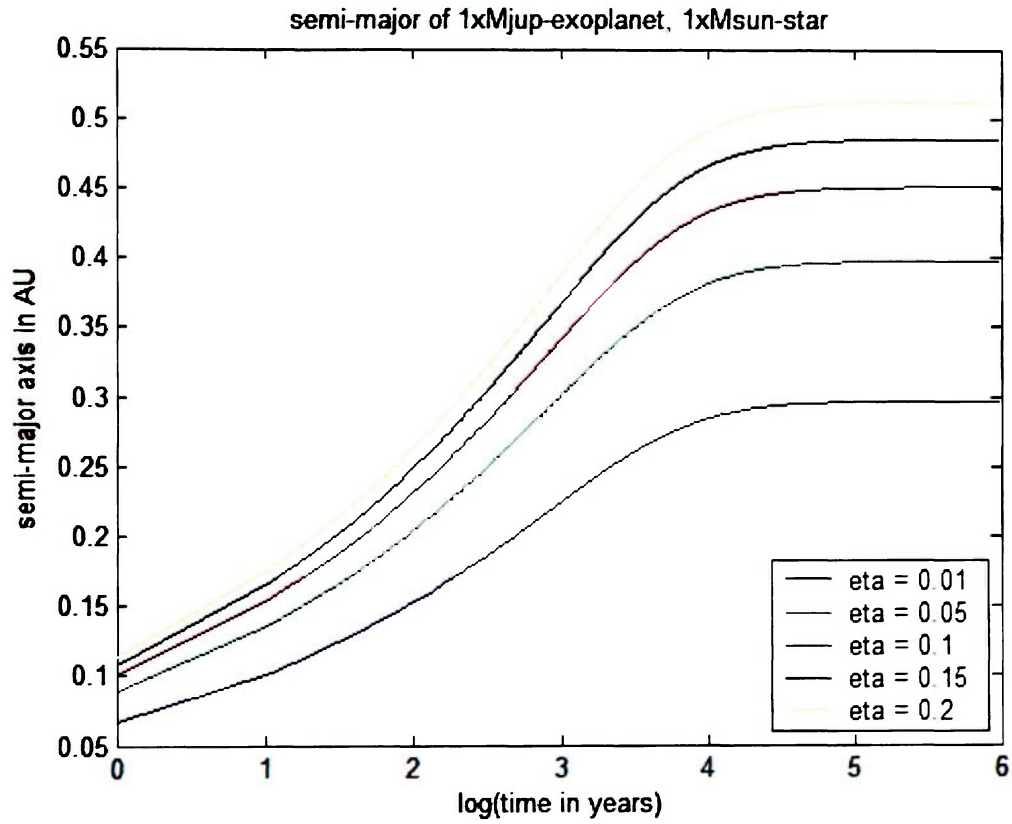


Figure 16. Time Development of Semimajor Axis for a  $M_{Jup}$  Size Planet about a  $M_{sun}$  Central Star [ $B_o = 5$  kG;  $e = 0.0$ ;  $\gamma = 1$ ;  $a_o = 0.04$  AU].

### ***D. Eccentricity of the Orbiting Planet***

The maximum eccentricity of an extrasolar planet found today is 0.93 with an overall average of approximately 0.25. However, most eccentricities for the hot Jupiter planets are basically 0.0 due to their circularized locked orbits. The effect of low eccentricity values was calculated for the planet-star system previously described. Figure 17 displays the results of the final semimajor axis calculation, and, as suspected, the variation is minimal.

### ***E. Surface Magnetic Field Strength***

A star's dipole magnetic field weakens with distance  $r$  from the surface as  $r^{-3}$ . In addition, the magnetic field of a star weakens with age from a highly magnetized ( $B_o = 5$  kG) during the T-Tauri phase to low magnetism ( $B_o = 5$  G) on the main-sequence star. On the timescale for planet formation and migration, the central star will remain strongly magnetized so that Figure 18 displays the calculation for variation in the star's surface magnetic field  $B_o$  ranging between 1 and 5 kilogauss. As expected, the higher the magnetic field, the stronger the torque. Since  $B_o$  is squared in the magnetic torque term, affecting the combined poloidal and toroidal field contributions, the results are more sensitive to varying magnetic field strength than from other parameters such as eccentricity or the flux tube area fraction  $\eta$ . This distribution is due to the power law variation and therefore is a strong parameter to be considered along with the star's mass and overall size.

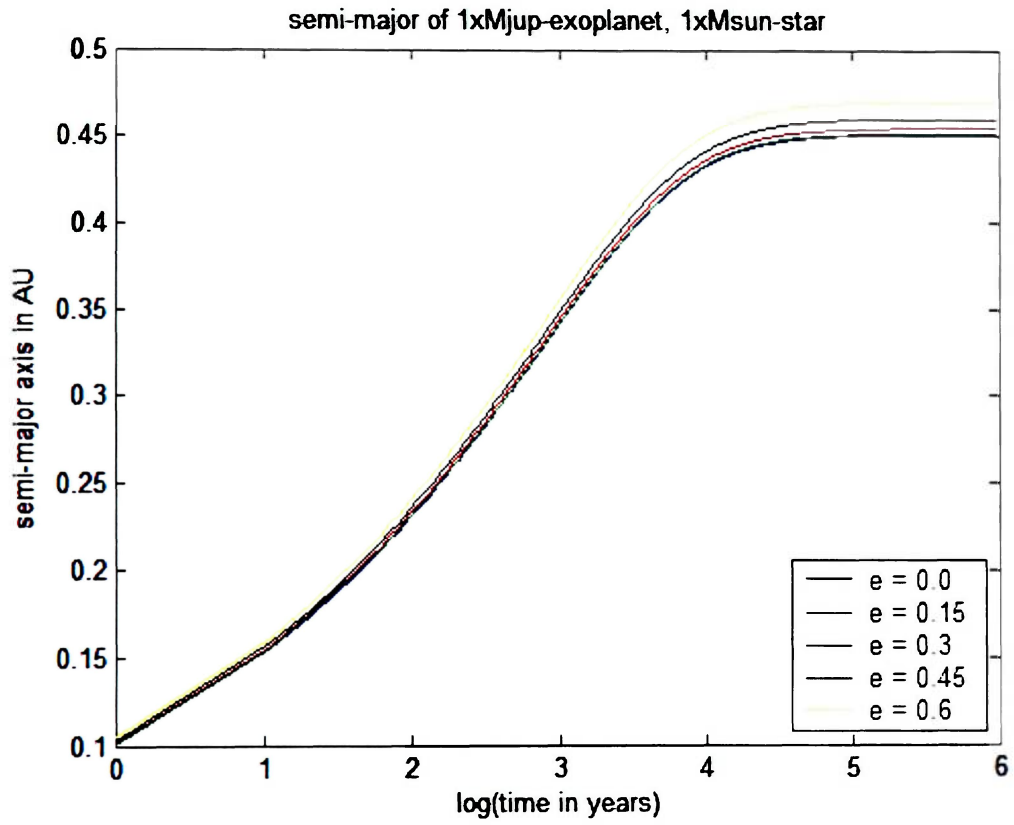


Figure 17. Time Development of Semimajor Axis for a  $M_{Jup}$  Size Planet about a  $M_{sun}$  Central Star [ $B_o = 5$  kG;  $a_o = 0.04$  AU;  $\gamma = 1.0$ ;  $\eta = 0.1$ ].

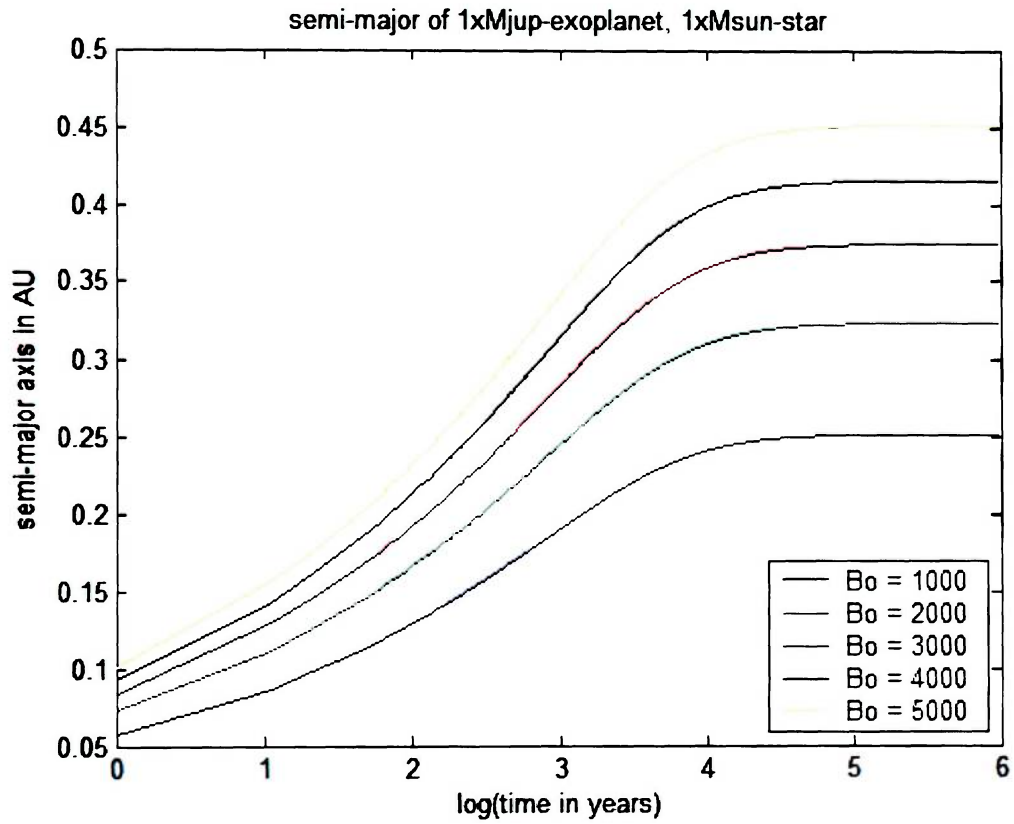


Figure 18. Time Development of Semimajor Axis for a  $M_{Jup}$  Size Planet about a  $M_{sun}$  Central Star [ $e = 0.0$ ;  $\gamma = 1.0$ ;  $\eta = 0.1$ ;  $a_o = 0.04$  AU].

## ***F. Initial Semimajor Axis***

The initial semimajor axis of an orbiting planet in these calculations is an artificial condition that results from starting the time step after the planet has already formed and migrated inward. Since the planet would already be experiencing the outward push of the magnetic torque as it begins its close approach to the star, there exists some error in assuming that the magnetic torque suddenly turns on at time  $t = 0$  in this calculation. Therefore, Figure 19 examines the range of semimajor axis in which the magnetic torque is strong enough to make changes in the planet's distance from the central star. It can be seen that as the planet is pushed out past the orbital distance of Venus and approaches that of Earth ( $a = 1$  AU), the magnetic torque rapidly loses its strength from the dipole field drop off. As previously stated, an advantage to using the dipole field approximation is that it is the weakest magnetic field topology that can be used, so the field may be stronger than modeled here; however, it is clear that there is an outer limit within which the planet must have migrated before the magnetic torque has a strong influence.

Overall, all the calculations presented here show a range of changes in the semimajor axis of an orbiting planet between 0.25 AU and 0.55 AU. The most influential parameters governing the planet's position are the star's properties itself – the mass and therefore size of the star. In addition, the star's surface magnetic field strength and the planet's initial semimajor axis had strong influences on the calculations. Other parameters such as the “twist” parameter of the toroidal and poloidal magnetic field components ( $\gamma$ ) and the planet's mass, area of magnetic flux tube interception, and eccentricity, had only minor influences on the planet's orbital progression with time.



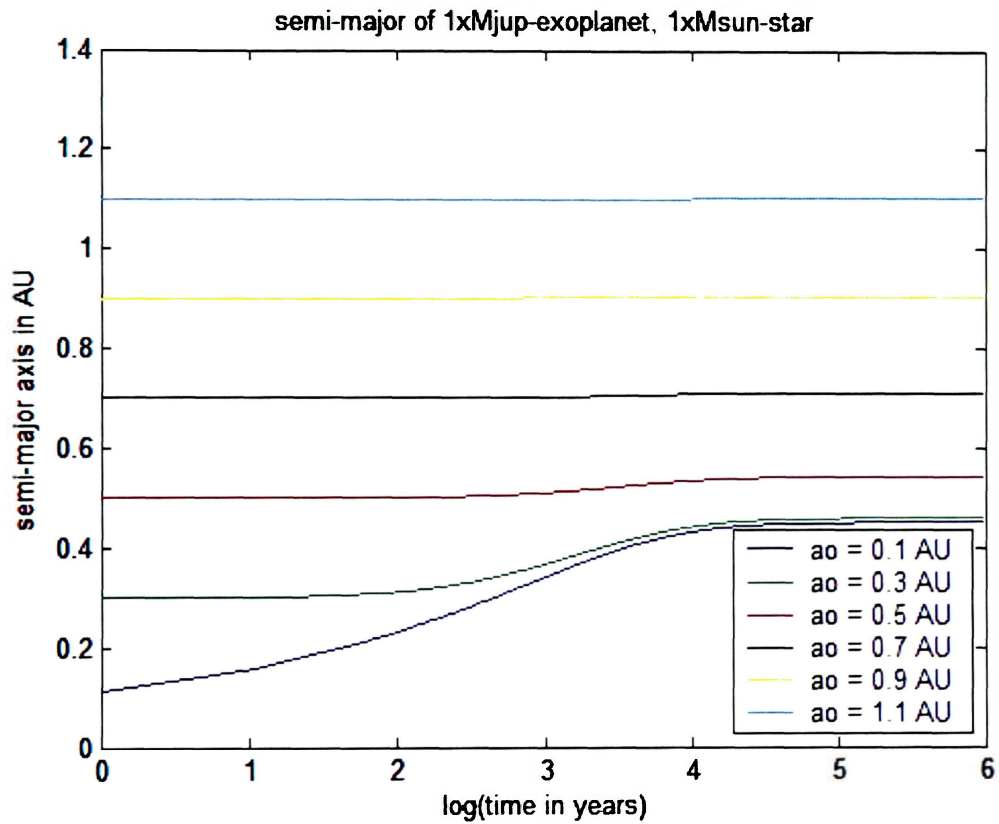


Figure 19. Time Development of Semimajor Axis of a  $M_{Jup}$  Size Planet about a  $M_{sun}$  Central Star for Varying Initial Semimajor Axis Positions [ $e = 0.0$ ;  $\gamma = 1.0$ ;  $\eta = 0.1$ ;  $B_o = 5$  kG].

## VII. Conclusion

Over the past decade, the search for extrasolar planets has uncovered an interesting trend in the orbital period of nearly 20% of the planets found; they are gas giant planets with roughly 3 day orbital periods. This observed planet “pile-up” has previously been thought to be due to the tidal torque the planet has with the central star. Although this may be a contributing factor, the dissipation parameter  $Q_{st}$  is so uncertain that the effectiveness of this mechanism is brought into question. This research proposed is an alternative torque which may be responsible, or partially responsible, for the halt in the migration of these Type II planets, namely the magnetic torque the star’s magnetic field imposes on the planet as it orbits the central star.

The semimajor axis for a single orbiting planet about a central star was calculated and evaluated in this study. The central star was considered to have a magnetic dipole field and to be a fast rotator during the pre-main-sequence phase of its evolution. The contraction of the star was considered since the dipole field depends strongly on the radius of the star. Using the data from D’Antona & Mazzitelli (1994) the radii for four different central star masses,  $2M_{sun}$ ,  $1.5M_{sun}$ ,  $M_{sun}$ , and  $0.5M_{sun}$ , were calculated and then fit to the theoretical expression determined by Cameron (1995). After justifying that the planet had the minimum ionization required to be essentially “frozen” to the magnetic field lines of the star, the semimajor axis distribution results were presented in §VI.

The results showed that any planet that comes within a few tenths of an AU of its star will be under a strong influence of a magnetic braking torque. The field weakens with time as the radius of the star contracts and the planets settle into a final position by

approximately 1 Myrs. The range of final semimajor axis location was between 0.25 AU and 0.55 AU. The most influential factor in determining the strength of the magnetic torque was the central star's own properties. Since a star's radius depends on its mass, the central star mass showed the most sensitivity in how far out it pushed a planet, with smaller stars being less efficient than massive stars, as expected.

A more complete analysis of migrating planets should combine the magnetic and tidal torques together would prove the most effective outward torque on the planet. If this were coupled and balanced with the inward migration models that are currently being discussed, the true time-dependent semimajor axis of the planet's orbit could be found. It is no surprise that the values found in this study are much larger than the true hot Jupiter locations because the inward forces were not considered.

In a more complex environment, the magnetic torque effect outside the equatorial plane could be calculated, utilizing a full magnetohydrodynamic model. In addition, since multi-planet systems are now known to be not uncommon, considering these effects for planet-star systems in which there are three or more bodies versus only two studied here, would seem warranted. Nevertheless, this study has shown that the magnetic braking of a star on an orbiting protoplanet should not be discarded as a possible mechanism explaining the curious exoplanet period "pile-up" puzzling many astronomers today.

## VIII. References

- Alexander, D. R., Augason, G. C., & Johnson, H. R. 1989, *ApJ*, **345**, 1014  
Cameron, A. G. W., 1995, *Meteorites*, **30**, 133  
D'Antona, F., & Mazzitelli, I. 1994, *ApJSS*, **90**, 467  
de Pater, I., & Lissauer, J. J., *Planetary Sciences*, Cambridge University Press, 2001, pgs. 259-261  
Elmegreen, B. G., 1979, *ApJ*, **232**, 729  
Fleck, R. C., & Hunter, J. H., 1976, *Mon. Not. R. astr. Soc.*, **175**, 335  
Guillot, T., Burrows, A., Hubbard, W. B., Lunine, J. I., & Saumon, D., 1996, *ApJ*, **459**, L35  
Henyey, L., Vardya, M. S., & Bodenheimer, P. 1965 *ApJ*, **142**, 841  
Herbst, W., Bailer-Jones, C. A. L., Mundt, R., Meisenheimer, K., & Wackermann, R., 2002, *A&A*, **396**, 513  
Hoyle, F. 1960, *Q. Jl. R. astr. Soc.*, **1**, 28  
Kurucz, R. L. 1991, in *Stellar Atmospheres: Beyond the Classical Models*, ed. L. Crivellari, I. Hubeny, & D. G. Hummer (NATO ASI Ser.; Dordrecht: Kluwer), 441  
Lin, D. N. C., Bodenheimer, P., & Richardson, D. C. 1996, *Nature*, **380**, 606  
Lin, D. N. C., & Papaloizou J. C. B. 1986, *ApJ*, **309**, 846  
Lst, R., & Schliter, A. 1955, *Z. Astrophys.*, **38**, 190  
Matt, S., & Pudritz, R. E., 2005, *Mon. Not. R. Astron. Soc.*, **356**, 167  
Nakano, T., & Tademaru, E., 1972, *ApJ*, **173**, 87  
Nelson, R. P., & Papaloizou J. C. B. 2004, "Orbital Migration and Disc-Planet Interactions" in *Extrasolar Planets: Today and Tomorrow ASP Conference Series* **321**, 367  
Oppenheimer, M., & Dalgarno A., 1974, *ApJ*, **192**, 29  
Penz, T., Lammer, H., Lichtenegger, H. I. M., Biernat, H. K., Wurz, P., Grießmeimer, J. M., & Weiss, W. W., 2005, *ApJ*, **157**, 396  
Pudritz, R. E., & Silk, J., 1987, *ApJ*, **316**, 213  
Shang, H., Glassgold, A. E., Shu, F. H., & Lizano, S., 2001, *Amer. Astron. Soc.*, **33**, 824  
Skumanich, A. 1972, *ApJ*, **171**, 565  
Spitzer, Jr., L., *Diffuse Matter in Space*, John Wiley & Sons, Inc., 1968, pgs. 238 – 242  
Trilling, D. E., Benz, W., Guillot, T., Lunine, J. I., Hubbard, W., & Burrows, A. 1998, *ApJ*, **500**, 428  
Werner, M. W., 1970, *Astrophys. Letters*, **6**, 81  
Zanstra, H., 1954, *Observatory*, **74**, 66

Websites:

[www.obspm.fr/planets](http://www.obspm.fr/planets) - The Extrasolar Planets Encyclopedia March 11<sup>th</sup> 2006

## **APPENDIX A**

Extrasolar Planet Data Chart

Table 6. Planetary Properties (Schneider 2006) Updated March 11 2006.

Planet Name	Pl. Mass ( $M_{Jup}$ )	Pl. Period (days)	Pl. Semi-axis (AU)	Pl. Ecc	Pl. Incl (deg)	Ang. Dist (arcsec)
14 Her b	4.74	1796.4	2.8	0.34		0.155
16 Cyg B b	1.69	798.94	1.67	0.67		0.078
47 Uma b	2.54	1089	2.09	0.06		0.157
47 Uma c	0.76	2594	3.73	0.1		0.28
51 Peg b	0.47	4.23	0.05	0		0.004
55 Cnc b	0.78	14.67	0.12	0.02		0.009
55 Cnc c	0.22	43.93	0.24	0.44		0.018
55 Cnc d	3.92	4517.4	5.26	0.33		0.392
55 Cnc e	0.05	2.81	0.04	0.17		0.003
70 Vir b	7.44	116.69	0.48	0.4		0.022
BD-10 3166 b	0.48	3.49	0.05	0.07		
Epsilon Eridani b	0.86	2502.1	3.3	0.61		1.031
Gamma Cephei b	1.59	902.26	2.03	0.2		0.172
GJ 3021 b	3.32	133.82	0.49	0.51		0.028
GJ 436 b	0.07	2.64	0.03	0.12		0.003
Gl 581 b	0.06	5.37	0.04	0		0.007
Gl 86 b	4.01	15.77	0.11	0.05		0.01
Gliese 876 b	1.94	60.94	0.21	0.02	84	0.044
Gliese 876 c	0.56	30.1	0.13	0.27	84	0.028
Gliese 876 d	0.02	1.94	0.02	0		0.004
HD 101930 b	0.3	70.46	0.3	0.11		0.01
HD 102117 b	0.14	20.67	0.15	0.06		0.004
HD 102195 b	0.48	4.12	0.05	0.06		0.002
HD 104985 b	6.3	198.2	0.78	0.03		0.008
HD 106252 b	6.81	1500	2.61	0.54		0.07
HD 10647 b	0.91	1040	2.1	0.18		0.121
HD 10697 b	6.12	1077.91	2.13	0.11		0.071
HD 108147 b	0.4	10.9	0.1	0.5		0.003
HD 108874 b	1.36	395.4	1.05	0.07		0.015
HD 108874 c	1.02	1605.8	2.68	0.25		0.039
HD 109749 b	0.28	5.24	0.06	0.01		0.001
HD 111232 b	6.8	1143	1.97	0.2		0.068
HD 114386 b	0.99	872	1.62	0.28		0.058
HD 114729 b	0.82	1131.48	2.08	0.31		0.059
HD 114762 b	11.02	83.89	0.3	0.34		0.011
HD 114783 b	0.99	501	1.2	0.1		0.055
HD 117207 b	2.06	2627.08	3.78	0.16		0.115
HD 117618 b	0.19	52.2	0.28	0.39		0.007
HD 118203 b	2.13	6.13	0.07	0.31		0.001
HD 11964 b	0.11	37.82	0.23	0.15		0.007
HD 11977 b	6.54	711	1.93	0.4		0.029
HD 121504 b	0.89	64.6	0.32	0.13		0.007
HD 12661 b	2.3	263.6	0.83	0.35		0.022
HD 12661 c	1.57	1444.5	2.56	0.2		0.069
HD 128311 b	2.18	448.6	1.1	0.25		0.066

HD 128311 c	3.21	919	1.76	0.17		0.106
HD 130322 b	1.08	10.72	0.09	0.05		0.003
HD 13189 b	14	471.6	1.85	0.28		0.01
HD 134987 b	1.58	260	0.78	0.24		0.031
HD 136118 b	11.9	1209	2.3	0.37		0.044
HD 141937 b	9.7	653.22	1.52	0.41		0.045
HD 142 b	1	337.11	0.98	0.38		0.048
HD 142022 A b	4.4	1923	2.8	0.57		0.078
HD 142415 b	1.62	386.3	1.05	0.5		0.031
HD 147513 b	1	540.4	1.26	0.52		0.098
HD 149026 b	0.36	2.88	0.04	0	85.3	0.001
HD 149143 b	1.33	4.07	0.05	0.02		0.001
HD 150706 b	1	264	0.82	0.38		0.03
HD 154857 b	1.8	398.5	1.11	0.51		0.016
HD 160691 b	1.67	654.5	1.5	0.31		0.098
HD 160691 c	3.1	2986	4.17	0.57		0.273
HD 160691 d	0.04	9.55	0.09	0		0.006
HD 16141 b	0.23	75.56	0.35	0.21		0.01
HD 162020 b	13.75	8.43	0.07	0.28		0.002
HD 168443 b	7.2	58.12	0.29	0.53		0.009
HD 168443 c	17.1	1739.5	2.87	0.23		0.087
HD 168746 b	0.23	6.4	0.07	0.08		0.002
HD 169830 b	2.88	225.62	0.81	0.31		0.022
HD 169830 c	4.04	2102	3.6	0.33		0.099
HD 177830 b	1.28	391	1	0.43		0.017
HD 178911 B b	6.29	71.49	0.32	0.12		0.007
HD 179949 b	0.98	3.09	0.04	0.05		0.001
HD 183263 b	3.69	634.23	1.52	0.38		0.029
HD 187123 b	0.52	3.1	0.04	0.03		0.001
HD 188015 b	1.26	456.46	1.19	0.15		0.023
HD 188753A b	1.14	3.35	0.04	0		0.001
HD 189733 b	1.15	2.22	0.03	0	85.3	0.002
HD 190228 b	4.99	1127	2.31	0.43		0.035
HD 190360 b	1.5	2891	3.92	0.36		0.247
HD 190360 c	0.06	17.1	0.13	0.01		0.008
HD 192263 b	0.72	24.35	0.15	0		0.008
HD 195019 b	3.43	18.3	0.14	0.05		0.007
HD 196050 b	3	1289	2.5	0.28		0.053
HD 196885 b	1.84	386	1.12	0.3		0.034
HD 19994 b	2	454	1.3	0.2		0.058
HD 202206 b	17.4	255.87	0.83	0.44		0.018
HD 202206 c	2.44	1383.4	2.55	0.27		0.055
HD 20367 b	1.07	500	1.25	0.23		0.046
HD 2039 b	4.85	1192.58	2.19	0.68		0.024
HD 208487 b	0.45	123	0.49	0.32		0.011
HD 209458 b	0.69	3.52	0.05	0.07	86.1	0.001
HD 210277 b	1.24	435.6	1.1	0.45		0.05
HD 212301 b	0.45	2.46	0.04	0		0.001
HD 213240 b	4.5	951	2.03	0.45		0.05
HD 216435 b	1.49	1442.92	2.7	0.34		0.081

HD 216437 b	2.1	1294	2.7	0.34	0.102
HD 216770 b	0.65	118.45	0.46	0.37	0.012
HD 217107 b	1.37	7.13	0.07	0.13	0.002
HD 217107 c	2.1	3150	4.3	0.55	0.116
HD 219449 b	2.9	182	0.3		0.007
HD 222582 b	5.11	572	1.35	0.76	0.032
HD 23079 b	2.61	738.46	1.65	0.1	0.047
HD 23596 b	7.19	1558	2.72	0.31	0.052
HD 2638 b	0.48	3.44	0.04	0	0.001
HD 27442 b	1.28	423.84	1.18	0.07	0.065
HD 27894 b	0.62	17.99	0.12	0.05	0.003
HD 28185 b	5.7	383	1.03	0.07	0.026
HD 30177 b	9.17	2819.65	3.86	0.3	0.07
HD 330075 b	0.76	3.37	0.04	0	0.001
HD 33564 b	9.1	388	1.1	0.34	0.052
HD 33636 b	9.28	2447.29	3.56	0.53	0.124
HD 34445 b	0.58	126	0.51	0.4	0.011
HD 3651 b	0.2	62.23	0.28	0.63	0.026
HD 37124 b	0.61	154.46	0.53	0.06	0.016
HD 37124 c	0.6	843.6	1.64	0.14	0.05
HD 37124 d	0.66	2295	3.19	0.2	0.097
HD 37605 b	2.3	55	0.25	0.68	0.006
HD 38529 b	0.78	14.31	0.13	0.29	0.003
HD 38529 c	12.7	2174.3	3.68	0.36	0.087
HD 39091 b	10.35	2063.82	3.29	0.62	0.16
HD 40979 b	3.32	267.2	0.81	0.23	0.024
HD 41004 A b	2.3	655	1.31	0.39	0.031
HD 4203 b	1.65	400.94	1.09	0.46	0.014
HD 4208 b	0.8	812.2	1.67	0.05	0.049
HD 4308 b	0.05	15.56	0.11	0	0.005
HD 45350 b	1.79	890.76	1.92	0.78	0.039
HD 46375 b	0.25	3.02	0.04	0.04	0.001
HD 47536 b	4.96	712.13	1.61	0.2	0.013
HD 49674 b	0.11	4.95	0.06	0.16	0.001
HD 50499 b	1.71	2582.7	3.86	0.23	0.082
HD 50554 b	4.9	1279	2.38	0.42	0.077
HD 52265 b	1.13	118.96	0.49	0.29	0.017
HD 59686 b	5.25	303	0.91	0	0.01
HD 63454 b	0.38	2.82	0.04	0	0.001
HD 6434 b	0.48	22.09	0.15	0.3	0.004
HD 65216 b	1.21	613.1	1.37	0.41	0.04
HD 68988 b	1.9	6.28	0.07	0.14	0.001
HD 70642 b	2	2231	3.3	0.1	0.114
HD 72659 b	2.96	3177.4	4.16	0.2	0.081
HD 73256 b	1.87	2.55	0.04	0.03	0.001
HD 73526 b	2.9	188.3	0.66	0.39	0.007
HD 73526 c	2.5	377.8	1.05	0.14	0.011
HD 74156 b	1.86	51.64	0.29	0.64	0.005
HD 74156 c	6.17	2025	3.4	0.58	0.053
HD 75289 b	0.42	3.51	0.05	0.05	0.002



HD 76700 b	0.2	3.97	0.05	0.13		0.001
HD 80606 b	3.41	111.78	0.44	0.93		0.008
HD 81040 b	6.86	1001.7	1.94	0.53		0.06
HD 82943 b	1.75	441.2	1.19	0.22		0.043
HD 82943 c	2.01	219	0.75	0.36		0.027
HD 83443 b	0.41	2.99	0.04	0.08		0.001
HD 8574 b	2.23	228.8	0.76	0.4		0.017
HD 88133 b	0.22	3.41	0.05	0.11		0.001
HD 89307 b	2.73	3090	4.15	0.27		0.126
HD 89744 b	7.99	256.61	0.89	0.67		0.022
HD 92788 b	3.86	377.7	0.97	0.27		0.03
HD 93083 b	0.37	143.58	0.48	0.14		0.017
HD 99492 b	0.12	17.04	0.12	0.05		0.007
HIP 75458 b	8.64	550.65	1.34	0.71		0.043
HR 810 b	1.94	311.29	0.91	0.24		0.059
OGLE-TR-10 b	0.54	3.1	0.04	0	86.5	0
OGLE-TR-111 b	0.53	4.02	0.05	0	86.5	0
OGLE-TR-113 b	1.35	1.43	0.02	0		0
OGLE-TR-132 b	1.19	1.69	0.03	0	85	0
OGLE-TR-56 b	1.45	1.21	0.02	0	81	0
rho CrB b	1.04	39.85	0.22	0.04		0.013
Tau Boo b	3.9	3.31	0.05			0.003
TrES-1	0.61	3.03	0.04	0.14	88.2	0
Ups And b	0.69	4.62	0.06	0.01		0.004
Ups And c	1.89	241.5	0.83	0.28		0.062
Ups And d	3.75	1284	2.53	0.27		0.188

Table 7. Stellar Properties (Schneider 2006) Updated March 11 2006.

Planet Name	St. Dist (pc)	St. Spec. Type	St. Mass ( $M_{sun}$ )	St. [Fe/H]	St. Right Asc.	St. Decli.
14 Her b	18.1	K0 V	1	0.35	16 10 23	+43 49 18
16 Cyg B b	21.4	G2.5 V	1.01	0.09	19 41 51	+50 31 03
47 Uma b	13.3	G0V	1.03	-0.08	10 59 29	+40 25 46
47 Uma c	13.3	G0V	1.03	-0.08	10 59 29	+40 25 46
51 Peg b	14.7	G2 IV			22 57 27	+20 46 07
55 Cnc b	13.4	G8 V	1.03	0.29	08 52 37	+28 20 02
55 Cnc c	13.4	G8 V	1.03	0.29	08 52 37	+28 20 02
55 Cnc d	13.4	G8 V	1.03	0.29	08 52 37	+28 20 02
55 Cnc e	13.4	G8 V	1.03	0.29	08 52 37	+28 20 02
70 Vir b	22	G4 V	1.1	-0.03	13 28 26	+13 47 12
BD-10 3166 b		G4 V	1.1	0.5	10 58 28	-10 46 13
Epsilon Eridani b	3.2	K2 V	0.8	-0.1	03 32 55	-09 27 29
Gamma Cephei b	11.8	K2 V		0	23 39 20	+77 37 56
GJ 3021 b	17.6	G6 V	0.9	0.2	00 16 12	-79 51 04
GJ 436 b	10.2	M2.5	0.41	-0.03	11 42 11	+26 42 23
Gl 581 b	6.3	M3	0.31	-0.25	15 19 26	-07 43 20
Gl 86 b	11	K1V	0.79	-0.24	02 10 14	-50 50 00

Gliese 876 b	4.7	M4 V	0.32	0.02	22 53 13	-14 15 13
Gliese 876 c	4.7	M4 V	0.32	0.02	22 53 13	-14 15 13
Gliese 876 d	4.7	M4 V	0.32	0.02	22 53 13	-14 15 13
HD 101930 b	30.5	K1 V	0.74	0.17	11 43 30	-58 00 24
HD 102117 b	42	G6V	0.95	0.18	11 44 50	-58 42 13
HD 102195 b	29	K0V	0.93	-0.09	11 45 42	+02 49 17
HD 104985 b	102	G9 III	1.5	-0.35	12 05 15	+76 54 20
HD 106252 b	37.4	G0	1.05	-0.16	12 13 29	+10 02 29
HD 10647 b	17.3	F8V	1.07	-0.03	01 42 29	-53 44 27
HD 10697 b	30	G5 IV	1.1	0.15	01 44 55	+20 04 59
HD 108147 b	38.6	F8/G0 V	1.27	0.2	12 25 46	-64 01 19
HD 108874 b	68.5	G5	1	0.14	12 30 26	+22 52 47
HD 108874 c	68.5	G5	1	0.14	12 30 26	+22 52 47
HD 109749 b	59	G3 IV	1.2	0.25	12 37 16	-40 48 43
HD 111232 b	29	G8V	0.78	-0.36	12 48 51	-68 25 30
HD 114386 b	28	K3 V		-0.03	13 10 39	-35 03 17
HD 114729 b	35	G3 V	0.93	-0.22	13 12 44	-31 52 24
HD 114762 b	28	F9V	0.82	-0.5	13 12 19	+17 31 01
HD 114783 b	22	K0	0.92	0.33	13 12 43	-02 15 54
HD 117207 b	33	G8VI/V	1.04	0.27	13 29 21	-35 34 15
HD 117618 b	38	G2V	1.05	0.04	13 32 25	-47 16 16
HD 118203 b	88.6	K0	1.23	0.1	13 34 02	+53 43 42
HD 11964 b	34	G5	1.13		01 57 09	-10 14 32
HD 11977 b	66.5	G8.5 III	1.91	-0.21	01 54 56	-67 38 50
HD 121504 b	44.4	G2 V	1	0.16	13 57 17	-56 02 24
HD 12661 b	37.2	G6 V	1.07	0.29	02 04 34	+25 24 51
HD 12661 c	37.2	G6 V	1.07	0.29	02 04 34	+25 24 51
HD 128311 b	16.6	K0	0.8	0.08	14 36 00	+09 44 47
HD 128311 c	16.6	K0	0.8	0.08	14 36 00	+09 44 47
HD 130322 b	30	K0 V	0.79	-0.02	14 47 32	-00 16 53
HD 13189 b	185	K2 II	4.5		02 09 40	+32 18 59
HD 134987 b	25	G5 V	1.05	0.23	15 13 28	-25 18 33
HD 136118 b	52.3	F9 V	1.24	-0.07	15 18 55	-01 35 32
HD 141937 b	33.5	G2/G3 V	1	0.16	15 52 17	-18 26 09
HD 142 b	20.6	G1 IV	1.1	0.04	00 06 19	-49 04 30
HD 142022 A b	35.9	K0 V	0.99	0.19	16 10 15	-84 13 53
HD 142415 b	34.2	G1 V	1.03	0.21	15 57 40	-60 12 00
HD 147513 b	12.9	G3/G5V	0.92	-0.03	16 24 01	-39 11 34
HD 149026 b	78.9	G0 IV	1.3	0.36	16 30 29	+38 20 50
HD 149143 b	63	G0 IV	1.21	0.26	16 32 51	+02 05 05
HD 150706 b	27.2	G0		-0.13	16 31 17	+79 47 23
HD 154857 b	68.5	G5V	1.17	-0.23	17 11 15	-56 40 50
HD 160691 b	15.3	G3 IV-V	1.08	0.28	17 44 08	-51 50 02
HD 160691 c	15.3	G3 IV-V	1.08	0.28	17 44 08	-51 50 02
HD 160691 d	15.3	G3 IV-V	1.08	0.28	17 44 08	-51 50 02
HD 16141 b	35.9	G5 IV	1	0.22	02 35 19	-03 33 38
HD 162020 b	31.3	K2 V	0.7	0.01	17 50 38	-40 19 06
HD 168443 b	33	G5	1.01	0.1	18 20 04	-09 35 34
HD 168443 c	33	G5	1.01	0.1	18 20 04	-09 35 34
HD 168746 b	43.1	G5	0.92	-0.07	18 21 49	-11 55 21

HD 169830 b	36.3	F8 V	1.4	0.21	18 27 49	-29 49 00
HD 169830 c	36.3	F8 V	1.4	0.21	18 27 49	-29 49 00
HD 177830 b	59	K0	1.17	0	19 05 20	+25 55 14
HD 178911 B b	46.7	G5	0.87	0.28	19 09 03	+34 35 59
HD 179949 b	27	F8 V	1.24	0.02	19 15 33	-24 10 45
HD 183263 b	53	G2IV	1.17	0.3	19 28 24	+08 21 28
HD 187123 b	50	G5	1.06	0.16	19 46 57	+34 25 15
HD 188015 b	52.6	G5IV	1.08	0.29	19 52 04	+28 06 01
HD 188753A b	44.8	K0	1.06		19 54 58	+41 52 17
HD 189733 b	19.3	K1-K2		-0.03	20 00 43	+22 42 39
HD 190228 b	66.1	G5IV	1.3	-0.24	20 03 00	+28 18 24
HD 190360 b	15.9	G6 IV	0.96		20 03 37	+29 53 48
HD 190360 c	15.9	G6 IV	0.96		20 03 37	+29 53 48
HD 192263 b	19.9	K2 V	0.79	-0.2	20 13 59	-00 52 00
HD 195019 b	20	G3 IV-V	1.02	0	20 28 17	+18 46 12
HD 196050 b	46.9	G3 V	1.1	0	20 37 51	-60 38 04
HD 196885 b	33	F8IV	1.27		20 39 51	+11 14 58
HD 19994 b	22.4	F8 V	1.35	0.23	03 12 46	-01 11 45
HD 202206 b	46.3	G6 V	1.15	0.37	21 14 57	-20 47 21
HD 202206 c	46.3	G6 V	1.15	0.37	21 14 57	-20 47 21
HD 20367 b	27	G0		0.1	03 17 40	+31 07 37
HD 2039 b	89.8	G2/G3 IV-V	0.98	0.1	00 24 20	-56 39 00
HD 208487 b	45	G2V	1.3	-0.06	21 57 19	-37 45 49
HD 209458 b	47	G0 V	1.05	0.04	22 03 10	+18 53 04
HD 210277 b	22	G0	0.99	0.16	22 09 29	-07 32 32
HD 212301 b	52.7	F8 V			22 27 30	-77 43 04
HD 213240 b	40.8	G4 IV	1.22	0.23	22 31 00	-49 25 59
HD 216435 b	33.3	G0 V	1.25	0.15	22 53 37	-48 35 53
HD 216437 b	26.5	G4 IV-V	1.07	0	22 54 39	-70 04 25
HD 216770 b	38	K1 V	0.9	0.23	22 55 53	-26 39 31
HD 217107 b	37	G8 IV	0.98	0.3	22 58 15	-02 23 42
HD 217107 c	37	G8 IV	0.98	0.3	22 58 15	-02 23 42
HD 219449 b	45	K0 III			23 15 53	-09 05 15
HD 222582 b	42	G5	1	-0.01	23 41 51	-05 59 08
HD 23079 b	34.8	F8/G0 V	1.1		03 39 43	-52 54 57
HD 23596 b	52	F8		0.32	03 48 00	+40 31 50
HD 2638 b	53.7	G5	0.93	0.16	00 29 59	-05 45 50
HD 27442 b	18.1	K2 IV a	1.2	0.2	04 16 29	-59 18 07
HD 27894 b	42.4	K2 V	0.75	0.3	04 20 47	-59 24 39
HD 28185 b	39.4	G5	0.99	0.24	04 26 26	-10 33 02
HD 30177 b	55	G8 V	0.95	0.25	04 41 54	-58 01 14
HD 330075 b	50.2	G5	0.95		15 49 37	-49 57 48
HD 33564 b	21	F6 V	1.25	-0.12	05 22 33	+79 13 52
HD 33636 b	28.7	G0 V	0.99	-0.13	05 11 46	+04 24 12
HD 34445 b	48	G0	1.11		05 17 40	+07 21 12
HD 3651 b	11	K0 V	0.79	0.05	00 39 21	+21 15 01
HD 37124 b	33	G4 V	0.91	-0.32	05 37 02	+20 43 50
HD 37124 c	33	G4 V	0.91	-0.32	05 37 02	+20 43 50
HD 37124 d	33	G4 V	0.91	-0.32	05 37 02	+20 43 50
HD 37605 b	42.9	K0V	0.8	0.39	05 40 01	+06 03 38

HD 38529 b	42.4	G4 IV	1.39	0.31	05 46 34	+01 10 05
HD 38529 c	42.4	G4 IV	1.39	0.31	05 46 34	+01 10 05
HD 39091 b	20.6	G1 IV	1.1	0.09	05 37 09	-80 28 08
HD 40979 b	33.3	F8 V	1.08	0.19	06 04 29	+44 15 37
HD 41004 A b	42.5	K1 V	0.7	-0.09	05 59 49	-48 14 22
HD 4203 b	77.5	G5	1.06	0.22	00 44 41	+20 26 56
HD 4208 b	33.9	G5 V	0.93	-0.24	00 44 26	-26 30 56
HD 4308 b	21.9	G5 V	0.83	-0.31	00 44 39	-65 38 58
HD 45350 b	49	G5 IV	1.02	0.29	06 28 45	+38 57 46
HD 46375 b	33.4	K1 IV	1	0.25	06 33 12	+05 27 46
HD 47536 b	123	KO II	1.1		06 37 47	-32 20 23
HD 49674 b	40.7	G5 V	1	0.25	06 51 30	+40 52 03
HD 50499 b	47.3	G IV	1.27		06 52 02	-33 54 56
HD 50554 b	31	F8	1.1	0.02	06 54 42	+24 14 44
HD 52265 b	28	G0 V	1.13	0.11	07 00 18	-05 22 01
HD 59686 b	92	K2 III			07 31 48	+17 05 09
HD 63454 b	35.8	K4 V	0.8	0.11	07 39 21	-78 16 44
HD 6434 b	40.3	G3 IV	1	-0.52	01 04 40	-39 29 17
HD 65216 b	34.3	G5 V	0.92	-0.12	07 53 4	-63 38 50
HD 68988 b	58	G0	1.2	0.24	08 18 22	+61 27 38
HD 70642 b	29	G5 IV-V	1	0.16	08 21 28	-39 42 19
HD 72659 b	51.4	G0 V	0.95	-0.14	08 34 03	-01 34 05
HD 73256 b	36.5	G8/K0	1.05	0.29	08 36 23	-30 02 15
HD 73526 b	99	G6 V	1.02	0.28	08 37 16	-41 19 08
HD 73526 c	99	G6 V	1.02	0.28	08 37 16	-41 19 08
HD 74156 b	64.6	G0	1.05	0.13	08 42 25	+04 34 41
HD 74156 c	64.6	G0	1.05	0.13	08 42 25	+04 34 41
HD 75289 b	28.9	G0 V	1.05	0.29	08 47 40	-41 44 12
HD 76700 b	59.7	G6 V	1		08 53 55	-66 48 03
HD 80606 b	58.4	G5	0.9	0.43	09 22 37	+50 36 13
HD 81040 b	32.6	G2/G3	0.96	-0.16	09 23 47	+20 21 52
HD 82943 b	27.5	G0	1.15	0.27	09 34 50	-12 07 46
HD 82943 c	27.5	G0	1.15	0.27	09 34 50	-12 07 46
HD 83443 b	43.5	K0 V	0.79	0.33	09 37 11	-43 16 19
HD 8574 b	44.2	F8		-0.09	01 25 12	+28 34 00
HD 88133 b	74.5	G5 IV	1.2	0.34	10 10 07	+18 11 12
HD 89307 b	33	G0V	1.27		10 18 21	+12 37 15
HD 89744 b	40	F7 V	1.4	0.18	10 22 10	+41 13 46
HD 92788 b	32.8	G5	1.06	0.24	10 42 48	-02 11 01
HD 93083 b	28.9	K3 V	0.7	0.15	10 44 20	-33 34 37
HD 99492 b	18	K2V	0.78	0.36	11 26 46	+03 00 22
HIP 75458 b	31.5	K2 III	1.05	0.03	15 24 55	+58 57 57
HR 810 b	15.5	G0V peculiar		0.25	02 42 31	-50 48 12
OGLE-TR-10 b	1500	G or K	1.22	0.12	17 51 28	-29 52 34
OGLE-TR-111 b	1500	G or K	0.82	0.12	10 53 1	-61 24 20
OGLE-TR-113 b	1500	K	0.77	0.14	10 52 24	-61 26 48
OGLE-TR-132 b	1500	F	1.35	0.43	10 50 34	-61 57 25
OGLE-TR-56 b	1500	G	1.04		17 56 35	-29 32 21
rho CrB b	16.7	G0V or G2V	0.95	-0.19	16 01 03	+33 18 51
Tau Boo b	15	F7 V	1.3	0.28	13 47 17	+17 27 22

TrES-1	157	K0V	0.87	0	19 04 09	+36 37 57
Ups And b	13.5	F8 V	1.3	0.09	01 36 48	+41 24 38
Ups And c	13.5	F8 V	1.3	0.09	01 36 48	+41 24 38
Ups And d	13.5	F8 V	1.3	0.09	01 36 48	+41 24 38

## **APPENDIX B**

Computer Code for the Calculation of Stellar Radius  
Done in MatLAB

```

%Brooke Alarcon
%Pre-MS radii calculation
%January 25th 2006
%Edits
%March 28th 2006

clear
clc
format long

%Constants
Lsun = 3.83e33;    %Solar Luminosity, egrs per second
Rsun = 6.96e10;   %Solar Radii, centimeters
s = 5.67e-5;      %Stephan-Boltzman Constant, ergs per
                  second*centimeter*Kelvin^4

t =
[7e4;1e5;2e5;3e5;5e5;7e5;1e6;2e6;3e6;5e6;7e6;1e7;2e7;3e7;5e7;7e7;1e8];
%Time progression in years
dt = 31557600;    %Number of seconds in a year
t2 = dt*t;       %Time progression in seconds

%Alexander + Rogers & Iglesias Opacities, CM Convection (a=0.5), Y =
0.28, Z=0.019
%Stellar Radii progression with time
%Matrix Columns [2.0; 1.5; 1.0; 0.5]Msun

%log(Lstar/Lsun)
logLA = [1.657 1.461 1.161 0.614;
1.552 1.392 1.125 0.563;
1.295 1.124 0.893 0.492;
1.162 0.984 0.733 0.339;
1.005 0.820 0.551 0.079;
0.908 0.714 0.438 -0.067;
0.810 0.606 0.319 -0.211;
0.671 0.409 0.090 -0.473;
0.683 0.320 -0.042 -0.598;
1.202 0.285 -0.193 -0.738;
1.132 0.386 -0.267 -0.827;
1.205 0.779 -0.307 -0.921;
1.204 0.695 -0.169 -1.105;
1.205 0.686 -0.038 -1.206;
1.208 0.688 -0.156 -1.384;
1.212 0.689 -0.150 -1.360;
1.217 0.692 -0.145 -1.384];

%log(Teff)
logTA = [3.683 3.677 3.665 3.629;
3.688 3.679 3.666 3.629;
3.699 3.689 3.672 3.628;
3.704 3.693 3.674 3.625;
3.709 3.697 3.675 3.616;
3.712 3.698 3.675 3.609;
3.714 3.700 3.673 3.601;
3.723 3.701 3.666 3.582;
3.737 3.705 3.661 3.576;
3.804 3.719 3.655 3.572;

```

```

3.913 3.742 3.655 3.572;
3.962 3.788 3.663 3.572;
3.963 3.854 3.718 3.572;
3.963 3.855 3.762 3.573;
3.963 3.856 3.754 3.576;
3.962 3.856 3.755 3.580;
3.961 3.857 3.755 3.584];

for i=1:length(t)
    for j=1:4
        LA(i,j) = Lsun*10^logLA(i,j);      %solving for Lstar
        TA(i,j) = 10^logTA(i,j);          %solving for Teff
        RA(i,j) = sqrt(LA(i,j)/(4*pi*s*TA(i,j)^4))*(1/Rsun);
                                                %Stellar Radii
    end
end

LstarA(:, :) = LA(:, :);
LstarA;

TeffA(:, :) = TA(:, :);
TeffA;

RstarA(:, :) = RA(:, :);
RstarA;

%Matching the Cameron Radius fit with this data
T = 4600;          %Surface Temp of the star in kelvin
Ro2 = 16*Rsun;    %Star's initial radius in centimeters--M = 2Msun
Ro15 = 14*Rsun;   %Star's initial radius in centimeters--M = 1.5Msun
Ro1 = 12*Rsun;    %Star's initial radius in centimeters--M = 1Msun
Ro05 = 10*Rsun;   %Star's initial radius in centimeters--M = 0.5Msun
G = 6.67e-8;      %Universal Gravitational Constant dyn cm^2 g^-2
Msun = 1.989e33;  %Solar Mass in grams
Mstar = [2*Msun 1.5*Msun 1*Msun 0.5*Msun];      %Mass of Star in grams
t1 = 1*dt:dt*10^4:dt*10^8;                       %Time step in seconds
for i = 1:length(t1)
    r2(i) =
(1/Rsun)*((28*pi*s*T^4)/(G*(Mstar(1))^2)*t1(i)+(1/Ro2^3))^(1/3);
%Fit for Mstar = 2Msun
    r15(i) =
(1/Rsun)*((28*pi*s*T^4)/(G*(Mstar(2))^2)*t1(i)+(1/Ro15^3))^(1/3);
%Fit for Mstar = 1.5Msun
    r1(i) =
(1/Rsun)*((28*pi*s*T^4)/(G*(Mstar(3))^2)*t1(i)+(1/Ro1^3))^(1/3);
%Fit for Mstar = 1Msun
    r05(i) =
(1/Rsun)*((28*pi*s*T^4)/(G*(Mstar(4))^2)*t1(i)+(1/Ro05^3))^(1/3);
%Fit for Mstar = 0.5Msun
end

figure(1)
plot(log10(t(:)),RstarA(:,1),'pb')
hold on
plot(log10(t(:)),RstarA(:,2),'dr')
plot(log10(t(:)),RstarA(:,3),'*g')

```



```

plot(log10(t(:)),RstarA(:,4),'vk')
plot(log10(t1(:)/dt),r2(:),'b-')
plot(log10(t1(:)/dt),r15(:),'r:')
plot(log10(t1(:)/dt),r1(:),'g-.'')
plot(log10(t1(:)/dt),r05(:),'k--')
title('Pre-Main Sequence Stellar Radii Trends, Alexander model')
xlabel('log(time in years)')
ylabel('Stellar Radii in Rsun')
legend('2.0 Msun', '1.5 Msun', '1.0 Msun', '0.5 Msun')

%Kurucz + Rogers & Iglesias Opacities, CM Convection (a=2), Y = 0.28,
    Z=0.019
%Stellar Radii progression with time
%Matrix Columns [2.0; 1.5; 1.0; 0.5]Msun

%log(Lstar/Lsun)
logLK = [1.653 1.449 1.151 0.602;
    1.559 1.392 1.116 0.546;
    1.288 1.114 0.885 0.474;
    1.154 0.972 0.724 0.338;
    0.995 0.806 0.541 0.063;
    0.896 0.699 0.425 -0.094;
    0.800 0.588 0.302 -0.243;
    0.663 0.389 0.067 -0.458;
    0.671 0.299 -0.068 -0.562;
    1.168 0.263 -0.222 -0.695;
    1.123 0.344 -0.300 -0.785;
    1.205 0.719 -0.342 -0.883;
    1.204 0.691 -0.218 -1.074;
    1.205 0.678 -0.019 -1.180;
    1.208 0.681 -0.167 -1.293;
    1.212 0.682 -0.161 -1.344;
    1.217 0.685 -0.156 -1.373];

%log(Teff)
logTK = [3.680 3.673 3.662 3.624;
    3.687 3.677 3.663 3.623;
    3.695 3.684 3.667 3.621;
    3.699 3.687 3.668 3.617;
    3.703 3.689 3.669 3.605;
    3.705 3.690 3.667 3.595;
    3.708 3.690 3.664 3.584;
    3.718 3.690 3.655 3.578;
    3.731 3.694 3.648 3.580;
    3.788 3.709 3.640 3.582;
    3.911 3.730 3.639 3.584;
    3.962 3.776 3.646 3.585;
    3.963 3.851 3.700 3.586;
    3.963 3.853 3.753 3.587;
    3.963 3.854 3.748 3.589;
    3.962 3.854 3.748 3.591;
    3.961 3.854 3.749 3.593];

for i=1:length(t)
    for j=1:4
        LK(i,j) = Lsun*10^logLK(i,j); %solving for Lstar
        TK(i,j) = 10^logTK(i,j); %solving for Teff
        RK(i,j) = sqrt(LK(i,j)/(4*pi*s*TK(i,j)^4))*(1/Rsun);
    end
end

```

```

        %Stellar Radii
    end
end

LstarK(:, :) = LK(:, :);
LstarK;

TeffK(:, :) = TK(:, :);
TeffK;

RstarK(:, :) = RK(:, :);
RstarK;

figure(2)
plot(log10(t(:)), RstarK(:, 1), 'pb')
hold on
plot(log10(t(:)), RstarK(:, 2), 'dr')
plot(log10(t(:)), RstarK(:, 3), '*g')
plot(log10(t(:)), RstarK(:, 4), 'vk')
plot(log10(t1(:)/dt), r2(:), 'b-')
plot(log10(t1(:)/dt), r15(:), 'r:')
plot(log10(t1(:)/dt), r1(:), 'g-.'')
plot(log10(t1(:)/dt), r05(:), 'k--')
title('Pre-Main Sequence Stellar Radii Trends, Kurucz model')
xlabel('log(time in years)')
ylabel('Stellar Radii in Rsun')
legend('2.0 Msun', '1.5 Msun', '1.0 Msun', '0.5 Msun')

```

## **APPENDIX C**

Computer Code for the Calculation of the  
Conservation of Angular Momentum  
Done in MatLAB

```

%Brooke Alarcon
%Thesis Code
%Angular Momentum Calculation for planet
%March 23rd 2006

clear
clc
format long

%Define Constants
Msun = 1.989e33;           %Mass of the sun in grams
Mjup = 1898.6e24;         %Mass of Jupiter in grams
Rsun = 6.96e10;           %Radius of the sun in centimeters
wrr = 3;                  %angular velocity of a rapidly rotating T-Tauri
                           star in rad/day
G = 6.67e-8;              %gravitational constant in dyn cm^2 g^-2
AU = 1.496e13;            %Conversion from AU to centimeters
day = 86400;              %Conversion from days to seconds
f = 0.1;                  %perfect sphere fraction for moment of inertial
E = 0.0;                  %Eccentricity of orbiting planet
a = 0.01*AU:0.5*AU:5.51*AU; %Semimajor axis of orbiting planet in
                           centimeters
Mstar = 1*Msun;           %Mass of Star in grams
Mp = 1*Mjup;              %Mass of planet in grams
Rstar = 2*Rsun;           %Stellar radius in centimeters
wstar = wrr/day;         %angular velocity of star in rad/sec

%Calculate the Star's angular momentum
Lstar = f*Mstar*Rstar^2*wstar

%Calculate the planet's angular momentum as a function of semimajor
axis
for i = 1:length(a)
    Lpl(i) = Mp*sqrt(G*(1-E^2)*(Mp+Mstar)*a(i));
end

a(:)/AU
Lpl(:)

```

## **APPENDIX D**

Computer Code for the Calculation of Semimajor Axis  
Done in MatLAB

```

%Brooke Alarcon
%Thesis Code
%Semi-Major Axis integration and plots
%December 24th 2005
%Edit's made:
%January 17th 2006
%January 31st 2006
%February 1st 2006
%March 5th 2006
%March 28th 2006
%April 4th 2006

clear
clc
format long

%Define Constants
Lsun = 3.83e33; %Solar Luminosity, egrs per second
Rsun = 6.96e10; %Solar Radii, centimeters
Msun = 1.989e33; %Solar Mass in grams
Mjup = 1898e27; %Mass of Jupiter in grams
s = 5.67e-5; %Stephan-Boltzman Constant, ergs per
second*centimeter*Kelvin^4;
G = 6.67e-8; %Gravitational Constant in dyne cm^2 per g^2
gamma = 1; %relation between torodal and poloidal B-fields
eta = 0.1; %Footprint of magnetic field lines on planet
AU = 1.496e13; %Au to centimeters conversion

%Planetary/Star system properties
T = 4600; %Stellar Temperature in Kelvin
Ro = [16*Rsun 14*Rsun 12*Rsun 10*Rsun]; %Star's initial radius in
centimeters
Bo = 5000; %Magnetic Field of Star in gauss
Mstar = [2*Msun 1.5*Msun 1*Msun 0.5*Msun]; %Mass of Star in grams
Mp = 1*Mjup; %Mass of planet in grams
E = 0.0; %eccentricity of planet
ao = 0.01:0.1:0.41; %Initial semi-major axis in AU
to = 0; %Initial time in years
t = 1:10^1:10^6; %Time step in years
dt = 31556736; %second to year conversion

%calculation semi-major axis for a 0.5 solar mass star
for i = 1:length(t)
    for j = 1:length(ao)
        C05 = (28*pi*s*T^4*Ro(4)^3)/(G*(Mstar(4))^2);
        a05(i,j) =
(1/AU)*(((ao(j)*AU)^(11/2)+((33*gamma*eta*Bo^2*G^0.5*(Mstar(4))^2*Ro(4)
^5)/(140*Mp*(1-E^2)^0.5*...
(Mp+Mstar(4))^0.5*pi*s*T^4))*((C05*dt*to+1)^(-5/3)-
(C05*dt*t(i)+1)^(-5/3)))^(2/11));
    end
end

%calculation semi-major axis for a 1.0 solar mass star
for i = 1:length(t)
    for j = 1:length(ao)
        C1 = (28*pi*s*T^4*Ro(3)^3)/(G*(Mstar(3))^2);

```

```

        a1(1,j) =
(1/AU)*(((ao(j)*AU)^(11/2)+((33*gamma*eta*Bo^2*G^0.5*(Mstar(3))^2*Ro(3)
^5)/(560*Mp*(1-E^2)^0.5*...
(Mp+Mstar(3))^0.5*p1*s*T^4))*((C1*dt*to+1)^(-5/3)-(C1*dt*t(1)+1)^(-
5/3)))^(2/11));
    end
end

%calculation semi-major axis for a 1.5 solar mass star
for i = 1:length(t)
    for j = 1:length(ao)
        C15 = (28*p1*s*T^4*Ro(2)^3)/(G*(Mstar(2))^2);
        a15(1,j) =
(1/AU)*(((ao(j)*AU)^(11/2)+((33*gamma*eta*Bo^2*G^0.5*(Mstar(2))^2*Ro(2)
^5)/(560*Mp*(1-E^2)^0.5*...
(Mp+Mstar(2))^0.5*p1*s*T^4))*((C15*dt*to+1)^(-5/3)-(C15*dt*t(1)+1)^(-
5/3)))^(2/11));
    end
end

%calculation semi-major axis for a 2.0 solar mass star
for i = 1:length(t)
    for j = 1:length(ao)
        C2 = (28*p1*s*T^4*Ro(1)^3)/(G*(Mstar(1))^2);
        a2(1,j) =
(1/AU)*(((ao(j)*AU)^(11/2)+((33*gamma*eta*Bo^2*G^0.5*(Mstar(1))^2*Ro(1)
^5)/(560*Mp*(1-E^2)^0.5* ..
(Mp+Mstar(1))^0.5*p1*s*T^4))*((C2*dt*to+1) (-5/3)-(C2*dt*t(1)+1)^(-
5/3)))^(2/11));
    end
end

%Plotting
figure(1)
plot(log10(t(:)),a05(:,1),'b')
hold on
plot(log10(t(:)),a05(:,2),'g')
plot(log10(t(:)),a05(:,3),'r')
plot(log10(t(:)),a05(:,4),'k')
plot(log10(t(:)),a05(:,5),'y')
title('semi-major of 1xMjup-exoplanet, 0.5xMsun-star')
xlabel('log(time in years)')
ylabel('semi-major axis in AU')
legend('ao = 0.01 AU','ao = 0.11 AU','ao = 0.21 AU','ao = 0.31 AU', 'ao
= 0.41 AU')

figure(2)
plot(log10(t(:)),a1(:,1),'b')
hold on
plot(log10(t(:)),a1(:,2),'g')
plot(log10(t(:)),a1(:,3),'r')
plot(log10(t(:)),a1(:,4),'k')
plot(log10(t(:)),a1(:,5),'y')
title('semi-major of 1xMjup-exoplanet, 1xMsun-star')
xlabel('log(time in years)')
ylabel('semi-major axis in AU')

```

```
legend('ao = 0.01 AU', 'ao = 0.11 AU', 'ao = 0.21 AU', 'ao = 0.31 AU', 'ao  
= 0.41 AU')
```

```
figure(3)  
plot(log10(t(:)), a15(:,1), 'b')  
hold on  
plot(log10(t(:)), a15(:,2), 'g')  
plot(log10(t(:)), a15(:,3), 'r')  
plot(log10(t(:)), a15(:,4), 'k')  
plot(log10(t(:)), a15(:,5), 'y')  
title('semi-major of 1xMjup-exoplanet, 1.5xMsun-star')  
xlabel('log(time in years)')  
ylabel('semi-major axis in AU')  
legend('ao = 0.01 AU', 'ao = 0.11 AU', 'ao = 0.21 AU', 'ao = 0.31 AU', 'ao  
= 0.41 AU')
```

```
figure(4)  
plot(log10(t(:)), a2(:,1) 'b')  
hold on  
plot(log10(t(:)), a2(:,2), 'g')  
plot(log10(t(:)), a2(:,3) 'r')  
plot(log10(t(:)), a2(:,4) 'k')  
plot(log10(t(:)), a2(:,5), 'y')  
title('semi-major of 1xMjup-exoplanet, 2xMsun-star')  
xlabel('log(time in years)')  
ylabel('semi-major axis in AU')  
legend('ao = 0.01 AU', 'ao = 0.11 AU', 'ao = 0.21 AU', 'ao = 0.31 AU', 'ao  
= 0.41 AU')
```



```

%Brooke Alarcon
%Thesis Code
%Semi-Major Axis integration and plots
%December 24th 2005
%Edit's made:
%January 17th 2006
%January 31st 2006
%February 1st 2006
%March 5th 2006
%March 28th 2006
%March 29th 2006
%April 4th 2006

clear
clc
format long

%Define Constants
Lsun = 3.83e33; %Solar Luminosity, egrs per second
Rsun = 6.96e10; %Solar Radius, centimeters
Msun = 1.989e33; %Solar Mass in grams
Mjup = 1898e27; %Mass of Jupiter in grams
s = 5.67e-5; %Stephan-Boltzman Constant, ergs per
second*centimeter*Kelvin^4;
G = 6.67e-8; %Gravitational Constant in dyne cm^2 per g^2
gamma = 1; %relation between torodal and poloidal B-fields
eta = 0.1; %Footprint of magnetic field lines on planet
AU = 1.496e13; %Au to centimeters conversion

%Planetary/Star system properties
T = 4600; %Stellar Temperature in Kelvin
Ro = 12*Rsun; %Star's initial radius in centimeters
Bo = 5000; %Magnetic Field of Star in gauss
Mstar = 1*Msun; %Mass of Star in grams
Mp = [0.1*Mjup 1*Mjup 5*Mjup 10*Mjup]; %Mass of planet in grams
E = 0.0; %eccentricity of planet
ao = 0.01:0.1:0.41; %Initial semi-major axis in AU
to = 0; %Initial time in years
t = 1:10^1:10^6; %Time step in years
dt = 31556736; %second to year conversion

%calculation semi-major axis for a 1.0 solar mass star and 0.1 Jupiter
Mass
%planet
for i = 1:length(t)
    for j = 1:length(ao)
        C05 = (28*pi*s*T^4*Ro^3)/(G*(Mstar)^2);
        a05(i,j) =
(1/AU)*(((ao(j)*AU)^(11/2))+((33*gamma*eta*Bo^2*G^0.5*(Mstar)^2*Ro^5)/(1
40*Mp(1)*(1-E^2)^0.5*...
(Mp(1)+Mstar)^0.5*pi*s*T^4))*((C05*dt*to+1)^(-5/3)-
(C05*dt*t(i)+1)^(-5/3)))^(2/11));
    end
end

%calculation semi-major axis for a 1.0 solar mass star and 1.0 Jupiter
Mass

```

```

%planet
for i = 1:length(t)
    for j = 1:length(ao)
        C1 = (28*pi*s*T^4*Ro^3)/(G*(Mstar)^2);
        a1(i,j) =
(1/AU)*(((ao(j)*AU)^(11/2))+((33*gamma*eta*Bo^2*G^0.5*(Mstar)^2*Ro^5)/(5
60*Mp(2)*(1-E^2)^0.5*...
(Mp(2)+Mstar)^0.5*pi*s*T^4)))*((C1*dt*to+1)^(-5/3)-
(C1*dt*t(i)+1)^(-5/3)))^(2/11));
    end
end

%calculation semi-major axis for a 1.0 solar mass star and 5.0 Jupiter
Mass
%planet
for i = 1:length(t)
    for j = 1:length(ao)
        C15 = (28*pi*s*T^4*Ro^3)/(G*(Mstar)^2);
        a15(i,j) =
(1/AU)*(((ao(j)*AU)^(11/2))+((33*gamma*eta*Bo^2*G^0.5*(Mstar)^2*Ro^5)/(5
60*Mp(3)*(1-E^2)^0.5*...
(Mp(3)+Mstar)^0.5*pi*s*T^4)))*((C15*dt*to+1)^(-5/3)-
(C15*dt*t(i)+1)^(-5/3)))^(2/11));
    end
end

%calculation semi-major axis for a 1.0 solar mass star and 10.0 Jupiter
Mass
%planet
for i = 1:length(t)
    for j = 1:length(ao)
        C2 = (28*pi*s*T^4*Ro^3)/(G*(Mstar)^2);
        a2(i,j) =
(1/AU)*(((ao(j)*AU)^(11/2))+((33*gamma*eta*Bo^2*G^0.5*(Mstar)^2*Ro^5)/(5
60*Mp(4)*(1-E^2)^0.5*...
(Mp(4)+Mstar)^0.5*pi*s*T^4)))*((C2*dt*to+1)^(-5/3)-
(C2*dt*t(i)+1)^(-5/3)))^(2/11));
    end
end

%Plotting
figure(1)
plot(log10(t(:)),a05(:,1),'b')
hold on
plot(log10(t(:)),a05(:,2),'g')
plot(log10(t(:)),a05(:,3),'r')
plot(log10(t(:)),a05(:,4),'k')
plot(log10(t(:)),a05(:,5),'y')
title('semi-major of 0.1xMjup-exoplanet, 1xMsun-star')
xlabel('log(time in years)')
ylabel('semi-major axis in AU')
legend('ao = 0.01 AU','ao = 0.11 AU','ao = 0.21 AU','ao = 0.31 AU', 'ao
= 0.41 AU')

figure(2)
plot(log10(t(:)),a1(:,1) 'b')
hold on

```

```

plot(log10(t(:)),a1(:,2),'g')
plot(log10(t(:)),a1(:,3),'r')
plot(log10(t(:)),a1(:,4),'k')
plot(log10(t(:)),a1(:,5),'y')
title('semi-major of 1xMjup-exoplanet, 1xMsun-star')
xlabel('log(time in years)')
ylabel('semi-major axis in AU')
legend('ao = 0.01 AU','ao = 0.11 AU','ao = 0.21 AU','ao = 0.31 AU', 'ao
= 0.41 AU')

```

```

figure(3)
plot(log10(t(:)),a15(:,1),'b')
hold on
plot(log10(t(:)),a15(:,2),'g')
plot(log10(t(:)),a15(:,3),'r')
plot(log10(t(:)),a15(:,4),'k')
plot(log10(t(:)),a15(:,5),'y')
title('semi-major of 5xMjup-exoplanet, 1xMsun-star')
xlabel('log(time in years)')
ylabel('semi-major axis in AU')
legend('ao = 0.01 AU','ao = 0.11 AU','ao = 0.21 AU','ao = 0.31 AU', 'ao
= 0.41 AU')

```

```

figure(4)
plot(log10(t(:)),a2(:,1),'b')
hold on
plot(log10(t(:)),a2(:,2),'g')
plot(log10(t(:)),a2(:,3),'r')
plot(log10(t(:)),a2(:,4),'k')
plot(log10(t(:)),a2(:,5),'y')
title('semi-major of 10xMjup-exoplanet, 1xMsun-star')
xlabel('log(time in years)')
ylabel('semi-major axis in AU')
legend('ao = 0.01 AU','ao = 0.11 AU','ao = 0.21 AU','ao = 0.31 AU', 'ao
= 0.41 AU')

```

```

%Brooke Alarcon
%Thesis Code
%Semi-Major Axis integration and plots
%December 24th 2005
%Edit's made:
%January 17th 2006
%January 31st 2006
%February 1st 2006
%March 5th 2006
%March 28th 2006
%March 29th 2006
%April 4th 2006

clear
clc
format long

%Define Constants
Lsun = 3.83e33; %Solar Luminosity, egrs per second
Rsun = 6.96e10; %Solar Radii, centimeters
Msun = 1.989e33; %Solar Mass in grams
Mjup = 1898e27; %Mass of Jupiter in grams
s = 5.67e-5; %Stephan-Boltzman Constant, ergs per
second*centimeter*Kelvin^4;
G = 6.67e-8; %Gravitational Constant in dyne cm^2 per g^2
gamma = [0.1 0.5 1 1.5 2]; %relation between torodal and poloidal B-
fields
eta = 0.1; %Footprint of magnetic field lines on planet
AU = 1.496e13; %Au to centimeters conversion

%Planetary/Star system properties
T = 4600; %Stellar Temperature in Kelvin
Ro = 12*Rsun; %Star's initial radius in centimeters
Bo = 5000; %Magnetic Field of Star in gauss
Mstar = 1*Msun; %Mass of Star in grams
Mp = 1*Mjup; %Mass of planet in grams
E = 0.0; %eccentricity of planet
ao = 0.04; %Initial semi-major axis in AU
to = 0; %Initial time in years
t = 1:10^1:10^6; %Time step in years
dt = 31556736; %second to year conversion

%calculation semi-major axis for a 1.0 solar mass star and 1.0 Jupiter
Mass
%planet, varying gamma
for i = 1:length(t)
    for j = 1:length(gamma)
        C05 = (28*pi*s*T^4*Ro^3)/(G*(Mstar)^2);
        a05(i,j) =
(1/AU)*(((ao*AU)^(11/2)+((33*gamma(j))*eta*Bo^2*G^0.5*(Mstar)^2*Ro^5)/(1
40*Mp*(1-E^2)^0.5*...
(Mp+Mstar)^0.5*pi*s*T^4)))*((C05*dt*to+1)^(-5/3)-
(C05*dt*t(i)+1)^(-5/3))^(2/11));
    end
end

%Plotting

```

```
figure(1)
plot(log10(t(:)),a05(:,1),'b')
hold on
plot(log10(t(:)),a05(:,2),'g')
plot(log10(t(:)),a05(:,3),'r')
plot(log10(t(:)),a05(:,4),'k')
plot(log10(t(:)),a05(:,5),'y')
title('semi-major of 1xMjup-exoplanet, 1xMsun-star')
xlabel('log(time in years)')
ylabel('semi-major axis in AU')
legend('gamma = 0.1','gamma = 0.5','gamma = 1','gamma = 1.5', 'gamma =
2')
```

```

%Brooke Alarcon
%Thesis Code
%Semi-Major Axis integration and plots
%December 24th 2005
%Edit's made:
%January 17th 2006
%January 31st 2006
%February 1st 2006
%March 5th 2006
%March 28th 2006
%March 29th 2006
%April 4th 2006

clear
clc
format long

%Define Constants
Lsun = 3.83e33; %Solar Luminosity, egrs per second
Rsun = 6.96e10; %Solar Radiu, centimeters
Msun = 1.989e33; %Solar Mass in grams
Mjup = 1898e27; %Mass of Jupiter in grams
s = 5.67e-5; %Stephan-Boltzman Constant, ergs per
second*centimeter*Kelvin^4;
G = 6.67e-8; %Gravitational Constant in dyne cm^2 per g^2
gamma = 1; %relation between torodal and poloidal B-fields
eta = [0.01 0.05 0.1 0.15 0.2]; %Footprint of magnetic field lines
on planet
AU = 1.496e13; %Au to centimeters conversion

%Planetary/Star system properties
T = 4600; %Stellar Temperature in Kelvin
Ro = 12*Rsun; %Star's initial radius in centimeters
Bo = 5000; %Magnetic Field of Star in gauss
Mstar = 1*Msun; %Mass of Star in grams
Mp = 1*Mjup; %Mass of planet in grams
E = 0.0; %eccentricity of planet
ao = 0.04; %Initial semi-major axis in AU
to = 0; %Initial time in years
t = 1:10^1:10^6; %Time step in years
dt = 31556736; %second to year conversion

%calculation semi-major axis for a 1.0 solar mass star and 1.0 Jupiter
Mass
%planet, varying eta
for i = 1:length(t)
    for j = 1:length(eta)
        C05 = (28*pi*s*T^4*Ro^3)/(G*(Mstar)^2);
        a05(i,j) =
(1/AU)*(((ao*AU)^(11/2))+((33*gamma*eta(j)*Bo^2*G^0.5*(Mstar)^2*Ro^5)/(1
40*Mp*(1-E^2)^0.5*...
(Mp+Mstar)^0.5*pi*s*T^4)))*((C05*dt*to+1)^(-5/3))-
(C05*dt*t(i)+1)^(-5/3))^(2/11));
    end
end

%Plotting

```

```
figure(1)
plot(log10(t(:)),a05(:,1),'b')
hold on
plot(log10(t(:)),a05(:,2),'g')
plot(log10(t(:)),a05(:,3),'r')
plot(log10(t(:)),a05(:,4),'k')
plot(log10(t(:)),a05(:,5),'y')
title('semi-major of 1xMjup-exoplanet, 1xMsun-star')
xlabel('log(time in years)')
ylabel('semi-major axis in AU')
legend('eta = 0.01','eta = 0.05','eta = 0.1','eta = 0.15', 'eta = 0.2')
```

```

%Brooke Alarcon
%Thesis Code
%Semi-Major Axis integration and plots
%December 24th 2005
%Edit's made:
%January 17th 2006
%January 31st 2006
%February 1st 2006
%March 5th 2006
%March 28th 2006
%March 29th 2006
%April 4th 2006

clear
clc
format long

%Define Constants
Lsun = 3.83e33; %Solar Luminosity, egrs per second
Rsun = 6.96e10; %Solar Radiu, centimeters
Msun = 1.989e33; %Solar Mass in grams
Mjup = 1898e27; %Mass of Jupiter in grams
s = 5.67e-5; %Stephan-Boltzman Constant, ergs per
second*centimeter*Kelvin^4;
G = 6.67e-8; %Gravitational Constant in dyne cm^2 per g^2
gamma = 1; %relation between torodal and poloidal B-fields
eta = 0.1; %Footprint of magnetic field lines on planet
AU = 1.496e13; %Au to centimeters conversion

%Planetary/Star system properties
T = 4600; %Stellar Temperature in Kelvin
Ro = 12*Rsun; %Star's initial radius in centimeters
Bo = 5000; %Magnetic Field of Star in gauss
Mstar = 1*Msun; %Mass of Star in grams
Mp = 1*Mjup; %Mass of planet in grams
E = [0.0 0.15 0.3 0.45 0.6]; %eccentricity of planet
ao = 0.04; %Initial semi-major axis in AU
to = 0; %Initial time in years
t = 1:10^1:10^6; %Time step in years
dt = 31556736; %second to year conversion

%calculation semi-major axis for a 1.0 solar mass star and 1.0 Jupiter
Mass
%planet, varying eccentricity
for i = 1:length(t)
    for j = 1:length(E)
        C05 = (28*pi*s*T^4*Ro^3)/(G*(Mstar)^2);
        a05(i,j) =
(1/AU)*(((ao*AU)^(11/2)+((33*gamma*eta*Bo^2*G^0.5*(Mstar)^2*Ro^5)/(140*
Mp*(1-E(j))^2)^0.5*...
(Mp+Mstar)^0.5*pi*s*T^4))*((C05*dt*to+1)^(-5/3)-
(C05*dt*t(i)+1)^(-5/3)))^(2/11));
    end
end

%Plotting
figure(1)

```



```
plot(log10(t(:)),a05(:,1),'b')
hold on
plot(log10(t(:)),a05(:,2) 'g')
plot(log10(t(:)),a05(:,3),'r')
plot(log10(t(:)),a05(:,4),'k')
plot(log10(t(:)),a05(:,5),'y')
title('semi-major of 1xMjup-exoplanet, 1xMsun-star')
xlabel('log(time in years)')
ylabel('semi-major axis in AU')
legend('e = 0.0','e = 0.15','e = 0.3','e = 0.45', 'e = 0.6')
```

```

%Brooke Alarcon
%Thesis Code
%Semi-Major Axis integration and plots
%December 24th 2005
%Edit's made:
%January 17th 2006
%January 31st 2006
%February 1st 2006
%March 5th 2006
%March 28th 2006
%March 29th 2006
%April 4th 2006

clear
clc
format long

%Define Constants
Lsun = 3.83e33; %Solar Luminosity, egrs per second
Rsun = 6.96e10; %Solar Radius, centimeters
Msun = 1.989e33; %Solar Mass in grams
Mjup = 1898e27; %Mass of Jupiter in grams
s = 5.67e-5; %Stephan-Boltzman Constant, ergs per
second*centimeter*Kelvin^4;
G = 6.67e-8; %Gravitational Constant in dyne cm^2 per g^2
gamma = 1; %relation between toroidal and poloidal B-fields
eta = 0.1; %Footprint of magnetic field lines on planet
AU = 1.496e13; %Au to centimeters conversion

%Planetary/Star system properties
T = 4600; %Stellar Temperature in Kelvin
Ro = 12*Rsun; %Star's initial radius in centimeters
Bo = [1000 2000 3000 4000 5000]; %Magnetic Field of Star in gauss
Mstar = 1*Msun; %Mass of Star in grams
Mp = 1*Mjup; %Mass of planet in grams
E = 0.0; %eccentricity of planet
ao = 0.04; %Initial semi-major axis in AU
to = 0; %Initial time in years
t = 1:10^1:10^6; %Time step in years
dt = 31556736; %second to year conversion

%calculation semi-major axis for a 1.0 solar mass star and 1.0 Jupiter
Mass
%planet, varying Bo
for i = 1:length(t)
    for j = 1:length(Bo)
        C05 = (28*pi*s*T^4*Ro^3)/(G*(Mstar)^2);
        a05(i,j) =
(1/AU)*(((ao*AU)^(11/2)+((33*gamma*eta*Bo(j)^2*G^0.5*(Mstar)^2*Ro^5)/(1
40*Mp*(1-E^2)^0.5*...
(Mp+Mstar)^0.5*pi*s*T^4)))*((C05*dt*to+1)^(-5/3)-
(C05*dt*t(i)+1)^(-5/3)))^(2/11));
    end
end

%Plotting
figure(1)

```

```
plot(log10(t(:)),a05(:,1),'b')
hold on
plot(log10(t(:)),a05(:,2),'g')
plot(log10(t(:)),a05(:,3),'r')
plot(log10(t(:)),a05(:,4),'k')
plot(log10(t(:)),a05(:,5),'y')
title('semi-major of 1xMjup-exoplanet, 1xMsun-star')
xlabel('log(time in years)')
ylabel('semi-major axis in AU')
legend('Bo = 1000','Bo = 2000','Bo = 3000','Bo = 4000', 'Bo = 5000')
```

```

%Brooke Alarcon
%Thesis Code
%Semi-Major Axis integration and plots
%December 24th 2005
%Edit's made:
%January 17th 2006
%January 31st 2006
%February 1st 2006
%March 5th 2006
%March 28th 2006
%March 29th 2006
%April 4th 2006

clear
clc
format long

%Define Constants
Lsun = 3.83e33; %Solar Luminosity, egrs per second
Rsun = 6.96e10; %Solar Radii, centimeters
Msun = 1.989e33; %Solar Mass in grams
Mjup = 1898e27; %Mass of Jupiter in grams
s = 5.67e-5; %Stephan-Boltzman Constant, ergs per
second*centimeter*Kelvin^4;
G = 6.67e-8; %Gravitational Constant in dyne cm^2 per g^2
gamma = 1; %relation between torodal and poloidal B-fields
eta = 0.1; %Footprint of magnetic field lines on planet
AU = 1.496e13; %Au to centimeters conversion

%Planetary/Star system properties
T = 4600; %Stellar Temperature in Kelvin
Ro = 12*Rsun; %Star's initial radius in centimeters
Bo = 5000; %Magnetic Field of Star in gauss
Mstar = 1*Msun; %Mass of Star in grams
Mp = 1*Mjup; %Mass of planet in grams
E = 0.0; %eccentricity of planet
ao = 0.1:0.2:1.1; %Initial semi-major axis in AU
to = 0; %Initial time in years
t = 1:10^1:10^6; %Time step in years
dt = 31556736; %second to year conversion

%calculation semi-major axis for a 1.0 solar mass star and 1.0 Jupiter
Mass
%planet, varying ao
for i = 1:length(t)
    for j = 1:length(ao)
        C05 = (28*pi*s*T^4*Ro^3)/(G*(Mstar)^2);
        a05(i,j) =
(1/AU)*(((ao(j)*AU)^(11/2))+((33*gamma*eta*Bo^2*G^0.5*(Mstar)^2*Ro^5)/(1
40*Mp*(1-E^2)^0.5*...
(Mp+Mstar)^0.5*pi*s*T^4)))*((C05*dt*to+1)^(-5/3)-
(C05*dt*t(i)+1)^(-5/3)))^(2/11));
    end
end

%Plotting
figure(1)

```

```
plot(log10(t(:)),a05(:,1),'b')
hold on
plot(log10(t(:)),a05(:,2),'g')
plot(log10(t(:)),a05(:,3),'r')
plot(log10(t(:)),a05(:,4),'k')
plot(log10(t(:)),a05(:,5),'y')
plot(log10(t(:)),a05(:,6),'c')
title('semi-major of 1xMjup-exoplanet, 1xMsun-star')
xlabel('log(time in years)')
ylabel('semi-major axis in AU')
legend('ao = 0.1 AU','ao = 0.3 AU','ao = 0.5 AU','ao = 0.7 AU', 'ao =
0.9 AU', 'ao = 1.1 AU')
```